 CMES, vol.58, no.2, pp.185-219, 2010

Energetic Galerkin BEM for wave propagation Neumann exterior problems

A. Aimi[1], M. Diligenti[1] and S. Panizzi[1]

Abstract: In this paper we consider 2D wave propagation Neumann exterior problems reformulated in terms of a hypersingular boundary integral equation with retarded potential. Starting from a natural energy identity satisfied by the solution of the differential problem, the related integral equation is set in a suitable space-time weak form. Then, a theoretical analysis of the introduced formulation is proposed, pointing out the novelties with respect to existing literature results. At last, various numerical simulations will be presented and discussed, showing accuracy and stability of the space-time Galerkin boundary element method applied to the energetic weak problem.

Keywords: wave propagation, Neumann exterior problems, energy identity, hypersingular boundary integral equation, Galerkin boundary element method.

1 Introduction

Exterior wave propagation problems have become an interesting field of research in the last decades (see e.g. [Patlashenko and Givoli (2000); Premrov and Spacapan (2004); Chandrasekhar and Rao (2005); Chandrasekhar (2005); Tadeu, Godinho, Antonio and Amado Mendes (2007)]).) For what concerns the discretization of hyperbolic initial-boundary value problems rewritten in terms of boundary integral equations (BIEs), in principle, both frequency-domain and time-domain boundary element methods (BEMs) can be used (see e.g. among recent works [Frangi (1999, 2000); Moser, Antes and Beer (2005); Kielhorn and Schanz (2008); Schanz, Antes and Ruberg (2005); Soares Jr. and Mansur (2007)]). Most earlier contributions concerned direct formulations of BEM in the frequency domain, often using the Laplace or Fourier transforms and addressing wave propagation problems. After this transformation a standard boundary integral method for an elliptic (Helmholtz) problem is applied and then the transformation back to time domain employs special methods for the inversion of Laplace or Fourier transforms.

[1] Dept. of Mathematics, University of Parma, Italy.

On the other side, the consideration of the time-domain (transient) problem yields directly the unknown time-dependent quantities. In this case, the representation formula in terms of single layer and double layer potentials uses the fundamental solution of the hyperbolic partial differential equation and jump relations, giving rise to retarded BIEs. Usual numerical discretization procedures include collocation techniques and Laplace-Fourier methods coupled with Galerkin boundary elements in space. The convolution quadrature method for the time discretization has been developed in [Lubich (1988, 1994)]. It provides a straightforward way to obtain an efficient time stepping scheme using the Laplace transform of the kernel function, although stability and convergence are assured under strong regularity assumptions on problem data.

The application of Galerkin boundary elements in both space and time has been implemented by several authors but in this direction only the weak formulation due to Bamberger and Ha Duong [Bamberger and Ha Duong (1986); Ha Duong (1990, 2003)] furnishes genuine convergence results. During the last 20 years, the Bamberger and Ha Duong method has been successfully applied to many problems in transient wave propagations (see e.g. [Becache (1993); Becache and Ha Duong (1994); Ha Duong, Ludwig and Terrasse (2003)]). The technique they use to find the weak formulation and to prove stability results may be summarized in the following steps: Fourier-Laplace transform in time variable; uniform estimates with respect to complex frequencies of the corresponding Helmholtz problem; application of Paley-Wiener theorem and Parseval identity. In particular this final step provides a space-time weak formulation (see (2.11)) closely related to the energy functional of the wave equation, whose associated quadratic form turns out to be coercive with respect to a suitable weighted Sobolev norm. The only drawback of the method is that passage to complex frequencies leads to stability constants that grow exponentially in time, as stated in [Costabel (2004)]. We refer to the surveys [Costabel (1994, 2004)] for a more complete bibliography on the subject.

In this paper, we consider two-dimensional Neumann problems for a temporally homogeneous (normalized) scalar wave equation outside an obstacle Γ in the time interval $[0,T]$, reformulated as a hypersinguar BIE with retarded potential. We avoid the passage to complex frequencies by simply exploiting the well-known energy-flux relation satisfied by any solution u of the (real-valued) wave equation. From the energy identity, we obtain a natural quadratic form in the unknown density and we derive a suitable space-time weak formulation of the integral problem. We remark that the idea of introducing a space-time weak formulation for the transient wave problem based on the energy identity is not new. In fact, in [Ha Duong, Ludwig and Terrasse (2003)] it was already exploited to get a satisfactory stability result for the acoustic wave equation with the aid of an absorbing boundary condition. Unfortunately, the case of the Neumann problem, here considered, does not

lead to any natural coerciveness property and is much more difficult to be theoretically treated.
Hence, starting from the consideration that for suitable geometries of the obstacle, and owing to the finite speed of propagation property, the square root of the energy defines a norm, special attention is devoted to the investigation of the coerciveness properties of the energy functional: in Section 2 we analyze it, via Fourier transform, in the case of a flat obstacle. Then in Section 3 Galerkin BEM discretization applied to the space-time energetic weak problem is introduced. At last various numerical simulations will be presented and discussed in Section 4. We will compare, when possible, results obtained with the energetic Galerkin BEM with analogous literature results. Instabilities phenomena, which arise starting from classical L^2 weak formulation of the BIEs, as shown in [Becache (1993)], are never present in the energetic procedure, which appears to be accurate and stable. Brief conclusions are reported in Section 5.
We finally note that the present work is conceived as a completion of [Aimi, Diligenti, Guardasoni, Mazzieri and Panizzi (2009)], where the energetic procedure for the exterior Dirichlet wave propagation problem, reformulated in terms of a weakly singular BIE, was theoretically and numerically analyzed.

2 Two-dimensional wave equation

2.1 Neumann problem and its energetic weak formulation

We will consider a Neumann problem for the wave equation exterior to an open arc $\Gamma \subset \mathbb{R}^2$ that is the scattering problem by a crack in an unbounded elastic isotropic medium $\Omega = \mathbb{R}^2 \setminus \Gamma$. Let Γ^- and Γ^+ denote the lower and upper faces of the crack, respectively, and $\mathbf{n}$ the normal unit vector to Γ, oriented from Γ^- to Γ^+. As usual, the total displacement field can be represented as the sum of the incident field (the wave propagating without the crack) and the scattered field. In a three-dimensional elastic isotropic medium, there are three plane waves propagating in a fixed direction: the P wave, the SH wave and the SV wave. The two-dimensional antiplane problem corresponds to an incident SH wave, when all quantities are independent of the third component z (in particular, the crack has to be invariant with respect to z).
The scattered wave satisfies the following Neumann problem for the wave operator (without loss of generality we will consider a dimensionless problem which can be

obtained after an appropriate scaling of the units):

$$u_{tt} - \triangle u = 0, \qquad \mathbf{x} \in \mathbb{R}^2 \setminus \Gamma, t \in (0,T) \tag{2.1}$$

$$u(\mathbf{x},0) = u_t(\mathbf{x},0) = 0, \qquad \mathbf{x} \in \mathbb{R}^2 \setminus \Gamma \tag{2.2}$$

$$\frac{\partial u}{\partial \mathbf{n}}(\mathbf{x},t) = g(\mathbf{x},t), \qquad (\mathbf{x},t) \in \Sigma_T := \Gamma \times [0,T]. \tag{2.3}$$

In (2.1)-(2.3) the unknown function u stands for the third component of the displacement field and g is the datum, which is the opposite of the normal derivative of the incident wave along Γ, i.e. $g = -\frac{\partial u^I}{\partial \mathbf{n}}$.
Let us consider the double layer representation of the solution of (2.1)-(2.3):

$$u(\mathbf{x},t) = \int_\Gamma \int_0^t \frac{\partial}{\partial \mathbf{n}_{\boldsymbol{\xi}}} G(r,t-\tau)\,\phi(\boldsymbol{\xi},\tau)\,d\tau\,d\gamma_{\boldsymbol{\xi}}, \quad \mathbf{x} \in \mathbb{R}^2 \setminus \Gamma,\ t \in (0,T), \tag{2.4}$$

where $r = \|\mathbf{x} - \boldsymbol{\xi}\|_2$, $\phi = [u]$ is the jump of u along Γ and G is the forward fundamental solution of the two-dimensional wave operator, that is

$$G(r,t-\tau) = \frac{1}{2\pi} \frac{H[t-\tau-r]}{\sqrt{(t-\tau)^2 - r^2}}, \tag{2.5}$$

where $H[\cdot]$ is the Heaviside function.
Taking the normal derivative with respect to $\mathbf{x}$ of the double layer potential and using the assigned Neumann boundary condition (2.3), we obtain the space-time hypersingular BIE

$$\int_\Gamma \int_0^t \frac{\partial^2}{\partial\, \mathbf{n}_{\mathbf{x}} \partial \mathbf{n}_{\boldsymbol{\xi}}} G(r,t-\tau)\,\phi(\boldsymbol{\xi},\tau)\,d\tau\,d\gamma_{\boldsymbol{\xi}} = g(\mathbf{x},t), \qquad \mathbf{x} \in \Gamma, t \in (0,T), \tag{2.6}$$

in the unknown density function ϕ, which can be written with the compact notation

$$D\phi = g. \tag{2.7}$$

Note that the hypersingular integral operator D can be equivalently expressed in the following way:

$$D\phi(\mathbf{x},t) = -\int_\Gamma \frac{\partial^2 r}{\partial \mathbf{n}_{\mathbf{x}} \partial \mathbf{n}_{\boldsymbol{\xi}}} \int_0^t G(r,t-\tau) \left[\phi_t(\boldsymbol{\xi},\tau) + \frac{\phi(\boldsymbol{\xi},\tau)}{(t-\tau+r)} \right] d\tau\,d\gamma_{\boldsymbol{\xi}}$$

$$+ \int_\Gamma \frac{\partial r}{\partial \mathbf{n}_{\mathbf{x}}} \frac{\partial r}{\partial \mathbf{n}_{\boldsymbol{\xi}}} \int_0^t G(r,t-\tau) \left[\phi_{tt}(\boldsymbol{\xi},\tau) + 2\frac{\phi_t(\boldsymbol{\xi},\tau)}{(t-\tau+r)} + 3\frac{\phi(\boldsymbol{\xi},\tau)}{(t-\tau+r)^2} \right] d\tau\,d\gamma_{\boldsymbol{\xi}}. \tag{2.8}$$

Expression (2.8) can be obtained starting from the definition of the double layer operator

$$\int_\Gamma \int_0^t \frac{\partial G}{\partial \mathbf{n}_{\boldsymbol{\xi}}}(r,t-\tau)\phi(\boldsymbol{\xi},\tau)\,d\tau\, d\gamma_{\boldsymbol{\xi}} \tag{2.9}$$

and observing that

$$\begin{aligned}
\frac{\partial G}{\partial \mathbf{n}_{\boldsymbol{\xi}}}(r,t-\tau) &= \frac{\partial G}{\partial r}(r,t-\tau)\,\frac{\partial r}{\partial \mathbf{n}_{\boldsymbol{\xi}}} = \frac{1}{2\pi}\,\frac{\partial}{\partial r}\Big[\frac{1}{\sqrt{t-\tau+r}}\,\frac{H[t-\tau-r]}{\sqrt{t-\tau-r}}\Big]\,\frac{\partial r}{\partial \mathbf{n}_{\boldsymbol{\xi}}} \\
&= \frac{1}{2\pi}\Big[-\frac{1}{2}\,\frac{1}{\sqrt{(t-\tau+r)^3}}\,\frac{H[t-\tau-r]}{\sqrt{t-\tau-r}} + \frac{1}{\sqrt{t-\tau+r}}\,\frac{\partial}{\partial r}\,\frac{H[t-\tau-r]}{\sqrt{t-\tau-r}}\Big]\,\frac{\partial r}{\partial \mathbf{n}_{\boldsymbol{\xi}}} \\
&= \frac{1}{2\pi}\Big[-\frac{1}{2}\,\frac{1}{t-\tau+r}\,\frac{H[t-\tau-r]}{\sqrt{(t-\tau)^2-r^2}} + \frac{1}{\sqrt{t-\tau+r}}\,\frac{\partial}{\partial \tau}\,\frac{H[t-\tau-r]}{\sqrt{t-\tau-r}}\Big]\,\frac{\partial r}{\partial \mathbf{n}_{\boldsymbol{\xi}}}\,.
\end{aligned}$$

Now, considering the integration over $\Gamma\times(0,t)$ of the obtained final expression multiplied by $\phi(\boldsymbol{\xi},\tau)$, integrating by parts the term containing the derivative with respect to τ, one gets, up to the factor $-\frac{1}{2\pi}$,

$$\int_\Gamma \frac{\partial r}{\partial \mathbf{n}_{\boldsymbol{\xi}}} \int_0^t \Big\{\frac{1}{2}\,\frac{H[t-\tau-r]}{\sqrt{(t-\tau)^2-r^2}}\,\frac{\phi(\boldsymbol{\xi},\tau)}{t-\tau+r} + \frac{H[t-\tau-r]}{\sqrt{t-\tau-r}}\,\frac{\partial}{\partial \tau}\Big[\frac{\phi(\boldsymbol{\xi},\tau)}{\sqrt{t-\tau+r}}\Big]\Big\}\,d\tau\, d\gamma_{\boldsymbol{\xi}}\,;$$

expressing explicitly the time derivative of the second term in the integrand function, one finally deduces the following equivalent expression for (2.9):

$$-\int_\Gamma \frac{\partial r}{\partial \mathbf{n}_{\boldsymbol{\xi}}} \int_0^t G(r,t-\tau)\left[\phi_t(\boldsymbol{\xi},\tau) + \frac{\phi(\boldsymbol{\xi},\tau)}{(t-\tau+r)}\right] d\tau\, d\gamma_{\boldsymbol{\xi}}\,. \tag{2.10}$$

At this stage, considering the derivative of (2.10) with respect to $\mathbf{n}_{\mathbf{x}}$ and operating with the same arguments as before, after a cumbersome but easy calculation one obtains (2.8).

The main mathematical results on existence and uniqueness of the solution to problem (2.7) are due to Bamberger and Ha Duong [Bamberger and Ha Duong (1986); Ha Duong (1990, 2003)]. Their analysis is based on the following space-time weak formulation:

$$\int_0^{+\infty} e^{-2\sigma t} \int_\Gamma (D\phi)(\mathbf{x},t)\,\psi_t(\mathbf{x},t)\,d\gamma_{\mathbf{x}}\,dt = \int_0^{+\infty} e^{-2\sigma t} \int_\Gamma g(\mathbf{x},t)\,\psi_t(\mathbf{x},t)\,d\gamma_{\mathbf{x}}\,dt \tag{2.11}$$

where σ is a strictly positive parameter and ψ is any test function belonging to a suitable functional space. Under the restriction $\sigma \geq \sigma_0 > 0$, Bamberger and Ha

Duong provide optimal results in terms of regularity and stabilty of the associated bilinear form.

The crucial remark is that the above formulation is strictly related to the energy of the wave equation, which is defined as follows

$$\mathscr{E}(t,u) := \frac{1}{2}\int_{\mathbb{R}^2\setminus\Gamma}\left(\left(\frac{\partial u(\mathbf{x},t)}{\partial t}\right)^2 + |\nabla u(\mathbf{x},t)|^2\right) d\mathbf{x}.$$

In fact, after multiplying by u_t the equation (2.1), we get the identity

$$(u_{tt} - \triangle u)\, u_t = \frac{\partial}{\partial t}\left(\frac{1}{2}u_t^2 + \frac{1}{2}|\nabla u|^2\right) - \nabla_x \cdot (u_t \nabla u) = 0, \tag{2.12}$$

satisfied by any solution u of the (real-valued) wave equation. If we integrate by parts on $\mathbb{R}^2\setminus\Gamma\times[0,T]$ the equation (2.12), under Neumann boundary conditions, we obtain

$$\begin{aligned} 0 &= \int_0^T \int_{\mathbb{R}^2\setminus\Gamma}\left\{\frac{\partial}{\partial t}\left(\frac{1}{2}u_t^2 + \frac{1}{2}|\nabla u|^2\right) - \nabla_{\mathbf{x}}\cdot(u_t\nabla u)\right\} d\mathbf{x}dt \\ &= \mathscr{E}(T,u) - \int_0^T \int_\Gamma \left[\frac{\partial u}{\partial t}\right](\mathbf{x},t)\,\frac{\partial u}{\partial \mathbf{n}}(\mathbf{x},t)\, d\gamma_{\mathbf{x}}\, dt\,. \end{aligned} \tag{2.13}$$

Since, along Γ, the jump $\left[\frac{\partial u}{\partial t}\right]$ of the time derivative of u represents also the time derivative of the density function ϕ in (2.7) and since, owing to (2.7) and (2.3), we have $\frac{\partial u}{\partial \mathbf{n}} = D\phi$, the equation (2.13) may be written as follows

$$\mathscr{E}(T,u) = \int_0^T \int_\Gamma (D\phi)(\mathbf{x},t)\,\phi_t(\mathbf{x},t)\; d\gamma_{\mathbf{x}}\, dt\,. \tag{2.14}$$

Note that for $\phi = \psi$ in the bilinear form defined by the left hand side of (2.11), considering the limit for $\sigma \to 0$ and restricting the integration to a bounded time interval $[0,T]$, we get the energetic quadratic form (2.14).

From now on, we shall refer to the energetic weak formulation of the BIE (2.7), as the space-time weak problem related to (2.14) and defined as follows

$$a_{\mathscr{E}}(\phi,\eta) = < g, \eta_t >_{L^2(\Sigma_T)}$$

where

$$a_{\mathscr{E}}(\phi,\eta) := < D\phi\,,\, \eta_t >_{L^2(\Sigma_T)} = \int_0^T \int_\Gamma (D\phi)(\mathbf{x},t)\,\eta_t(\mathbf{x},t)\, d\gamma_{\mathbf{x}}\, dt \tag{2.15}$$

and η is a suitable test function belonging to the same functional space of ϕ.
The main motivation for our theoretical and numerical work on the BIE (2.7), is that, as far as we know, in every numerical implementation of energy related Galerkin methods for the transient wave equation, the parameter σ in (2.11) has always been set equal to 0. As shown above, this corresponds to the weak formulation (2.15) with associated quadratic functional $\mathscr{E}(T,u)$. In this case there are many examples showing evidence of numerical stability but no theoretical result is known[1].
In the following section we investigate the coerciveness properties of the nonnegative quadratic form $\mathscr{E}(T,u)$ (the energy at a fixed time T) and we show that, at least for a simple geometrical configuration, it is possible to obtain some stability results.

2.2 Analysis of the energy in the case of a flat obstacle

In order to apply the Fourier transform to the analysis, we restrict ourselves to the case of a flat obstacle, that is $\Gamma = \{(x,0) : x \in [0,L]\}$.
We start by considering a given function $\phi \in \mathscr{S}(\mathbb{R}^2)$ (the space of rapidly decreasing C^∞ functions) having support in $\Gamma \times [0,+\infty)$. Then we reinterpret the function u given by the representation formula (2.4), as the solution of the jump problem:

$$u_{tt} - u_{xx} - u_{yy} = 0 \qquad (x,y) \in \mathbb{R}^2 \setminus \Gamma, \quad t > 0, \tag{2.16}$$

$$[u]\,(x,0,t) = \phi(x,t) \qquad x \in \mathbb{R}, \quad t > 0, \tag{2.17}$$

$$\left[\frac{\partial u}{\partial y}\right](x,0,t) = 0 \qquad x \in \mathbb{R}, \quad t > 0, \tag{2.18}$$

$$u(x,y,0) = u_t(x,y,0) = 0, \qquad (x,y) \in \mathbb{R}^2. \tag{2.19}$$

In what follows, we denote by $\mathscr{F}_{x,t}$ the Fourier transform in x and t, with dual real variables ξ and ω and we shall write

$$\hat{u}(\xi,y,\omega) := \mathscr{F}_{x,t}(u)(\xi,y,\omega) = \frac{1}{2\pi}\int_{-\infty}^{+\infty}\int_0^{+\infty} e^{-i(x\xi+t\omega)}\,u(x,y,t)\,dt\,dx\,, \;\; y \neq 0,$$

$$\hat{\phi}(\xi,\omega) := \mathscr{F}_{x,t}(\phi)(\xi,\omega) = \frac{1}{2\pi}\int_0^{L}\int_0^{+\infty} e^{-i(x\xi+t\omega)}\,\phi(x,t)\,dt\,dx$$

or

$$\tilde{\phi}(\xi,t) \;:=\; \mathscr{F}_x(\phi)(\xi,t) = \frac{1}{\sqrt{2\pi}}\int_0^{L} e^{-ix\xi}\,\phi(x,t)\,dx\,, \qquad t \in \mathbb{R}^+,$$

[1] Stabilty results are known for absorbing boundary conditions such those considered in [Ha Duong, Ludwig and Terrasse (2003)]. In this case the energy turns out to be a coercive quadratic functional.

the Fourier transform with respect to x. We shall also need the analytic extension of the Fourier transform with respect to t, to the complex half-plane $\mathscr{Im}\, z < 0$[2]. That is, for $z = \omega - i\sigma$, $\sigma > 0$, we set

$$\hat{\phi}(\xi, z) := \frac{1}{2\pi} \int_0^L \int_0^{+\infty} e^{-i(x\xi + tz)}\, \phi(x,t)\, dt\, dx = \mathscr{F}_{x,t}(e^{-\sigma t}\phi)(\xi, \omega).$$

We recall the Parseval's identity, valid for (real-valued) functions f (or g) such that $e^{-\sigma t} f \in L^2(\mathbb{R}^2)$:

$$\int_{-\infty}^{\infty} \int_{-\infty}^{\infty} e^{-2\sigma t} f(x,t) g(x,t)\, dx dt = \int_{-\infty}^{\infty} d\xi \int_{-\infty}^{\infty} \hat{f}(\xi, z) \overline{\hat{g}(\xi, z)}\, d\omega. \tag{2.20}$$

If we perform a Fourier transformation of problem (2.16) - (2.19) with respect to x and t, we obtain the following differential problem in y, with jumps conditions for $y = 0$,

$$(\xi^2 - z^2)\hat{u} - \hat{u}_{yy} = 0 \qquad y \neq 0, \tag{2.21}$$

$$[\hat{u}]\,(\xi, 0, z) = \hat{\phi}(\xi, z), \tag{2.22}$$

$$\left[\frac{\partial \hat{u}}{\partial y}\right](\xi, 0, z) = 0. \tag{2.23}$$

To solve problem (2.21) - (2.23), we first fix the the determination of the complex square root of $\xi^2 - z^2$ by setting

$$\mathscr{Re}\sqrt{\xi^2 - (\omega - i\sigma)^2} > 0, \qquad \text{for } \sigma > 0. \tag{2.24}$$

Then the solutions of the differential equation (2.21) for $y > 0$, are given by

$$\hat{u}(\xi, y, z) = A(\xi, z) \exp\left[-y\sqrt{\xi^2 - z^2}\right] + B(\xi, z) \exp\left[y\sqrt{\xi^2 - z^2}\right].$$

In order to determine the unknown functions A and B, we remark that to avoid exponential growth in y we must set $B(\xi, z) \equiv 0$. Then, by continuity for $y \to 0^+$, $A(\xi, z) = \hat{u}^+(\xi, 0, z)$, where $\hat{u}^\pm = \lim_{y \to 0^\pm} \hat{u}$. Analogous considerations hold for $y < 0$. It follows that the unique (finite energy) solution of problem (2.21) - (2.23) is given by

$$\hat{u}(\xi, y, z) = \begin{cases} \hat{u}^+(\xi, 0, z) \exp\left[-y\sqrt{\xi^2 - z^2}\right] & y > 0, \\ \hat{u}^-(\xi, 0, z) \exp\left[y\sqrt{\xi^2 - z^2}\right] & y < 0. \end{cases} \tag{2.25}$$

[2] This analytic extension is justified by the Paley-Wiener theorem for causal functions, that is for functions vanishing for $t < 0$.

By differentiation in (2.25) and thanks to (2.18), we get for $y = 0$

$$\frac{\partial \hat{u}}{\partial y}(\xi, 0, z) = -\sqrt{\xi^2 - z^2}\,\hat{u}^+(\xi, 0, z) = \sqrt{\xi^2 - z^2}\,\hat{u}^-(\xi, 0, z),$$

thus $\hat{u}^+(\xi, 0, z) = -\hat{u}^-(\xi, 0, z)$ and

$$\frac{\partial \hat{u}}{\partial y}(\xi, 0, z) = \frac{1}{2}\sqrt{\xi^2 - z^2}\,[\hat{u}](\xi, 0, z).$$

Therefore we have the following representation of the integral operator D in Fourier variables

$$\widehat{D\phi}(\xi, z) = \frac{1}{2}\sqrt{\xi^2 - z^2}\,\hat{\phi}(\xi, z). \tag{2.26}$$

Owing to the representation (2.26) and the Parseval's identity (2.20) for $f = D\phi$ and $g = \psi_t$, we can give a meaning to the bilinear form introduced in (2.11)

$$\int_0^L \int_0^{+\infty} e^{-2\sigma t}(D\phi)(x,t)\,\psi_t(x,t)\,dt\,dx = \frac{1}{2}\int_{-\infty}^{+\infty}\int_{-\infty}^{+\infty} \sqrt{\xi^2 - z^2}\,\widehat{\phi}(\xi, z)\overline{\widehat{\psi_t}(\xi, z)}\,d\xi\, d\omega$$

for various functional spaces. We refer to the Ha Duong's paper [Ha Duong (1990)] where this bilinear form has been studied in great details. Here we only define the space $\mathscr{H}_\sigma$, $\sigma > 0$, of functions in $L^2(\mathbb{R}^2)$, having support in $\Gamma \times [0, +\infty)$ and such that

$$\int_{-\infty}^{+\infty}\int_{-\infty}^{+\infty} |z|\,(|z|^2 + \xi^2)^{1/2}\,|\hat{\phi}(\xi, z)|^2\,d\omega\, d\xi < \infty, \qquad z = \omega - i\sigma, \quad \sigma > 0.$$

Owing to (2.20) and the identity $\widehat{\psi_t}(\xi, z) = iz\,\widehat{\psi}(\xi, z)$, we obtain

$$\int_0^L \int_0^{+\infty} e^{-2\sigma t}(D\phi)(x,t)\,\psi_t(x,t)\,dt\,dx = \frac{1}{2}\int_{-\infty}^{+\infty}\int_{-\infty}^{+\infty} \sqrt{\xi^2 - z^2}\,\hat{\phi}(\xi, z)\overline{iz\,\hat{\psi}(\xi, z)}\,d\omega\, d\xi\,, \tag{2.27}$$

and it is easy to see that, for functions $\phi, \psi \in \mathscr{H}_\sigma$, the right-hand side integral in (2.27) is finite. In some cases, the exponential in the first term of formula (2.27), can be eliminated by a passage to the limit as $\sigma \to 0^+$, for instance by assuming that ϕ and ψ belong to $H^1_+(\mathbb{R};\, H^{1/2}_{00}(\Gamma)) \subset \mathscr{H}_\sigma$, $\sigma > 0$, where

$$H^1_+(\mathbb{R}; H^{1/2}_{00}(\Gamma)) = \{\phi \in H^1(\mathbb{R}; H^{1/2}_{00}(\Gamma)) : \phi(t, \cdot) = 0 \quad \text{for } t < 0\}.$$

We recall that $H^{1/2}_{00}(\Gamma)$ is a proper subspace of $H^{1/2}(\Gamma)$ with strictly finer topology. The main property of functions in $H^{1/2}_{00}(\Gamma)$ is that their extension to zero out of $[0, L]$

belongs to $H^{1/2}(\mathbb{R})$. In what follows, this extension will always be understood. For ϕ, $\psi \in H^1_+(\mathbb{R}; H^{1/2}_{00}(\Gamma))$, it is not difficult to see that both the integrals in (2.27) are dominated uniformly with respect to σ. Thus, by the Lebesgue's dominated convergence Theorem, for $\sigma \to 0^+$, we get

$$\int_0^L \int_0^{+\infty} (D\phi)(x,t)\psi_t(x,t)dtdx = \frac{1}{2}\int_{-\infty}^{+\infty}\int_{-\infty}^{+\infty} \sqrt{\xi^2-\omega^2}\,\hat{\phi}(\xi,\omega)\overline{i\,\omega\,\hat{\psi}(\xi,\omega)}d\omega d\xi. \tag{2.28}$$

Here the determination of the square root is obtained by continuity form (2.24) and is given by

$$\sqrt{\xi^2-\omega^2} = \begin{cases} \sqrt{\xi^2-\omega^2} & |\xi| \geq |\omega|, \\ i\,\mathrm{sign}(\omega)\sqrt{\omega^2-\xi^2} & |\xi| < |\omega|. \end{cases} \tag{2.29}$$

This passage to the limit $\sigma \to 0^+$ has been studied by Lebeau and Schatzman in the paper [Lebeau and Schatzman (1984)], to which we refer for more details.
To obtain a Fourier representation from formula (2.28) of the energy $\mathscr{E}(T,u)$, of the solution u to the problem (2.16) - (2.19), we need: (i) to set $\psi = \phi$; (ii) to localize ϕ to a fixed time interval $[0,T]$. We note that the regularity required to the functions involved, does not allow us to simply truncate to zero ϕ for $t > T$, unless $\phi \in H^1_0([0,T]; H^{1/2}_{00}(\Gamma))$, that is $\phi(\cdot,0) = \phi(\cdot,T) = 0$. In this case, the trivial extension of ϕ out of $[0,T]$ is still in the functional space $H^1_+([0,T]; H^{1/2}_{00}(\Gamma))$. Thus for $\phi \in H^1_0([0,T]; H^{1/2}_{00}(\Gamma))$, (2.28) provides a formula for the energy $\mathscr{E}(T,u)$:

$$\begin{aligned} a_{\mathscr{E}}(\phi,\phi) &= \int_0^L \int_0^T (D\phi)(x,t)\phi_t(x,t)dtdx \\ &= \frac{-i}{2}\int_{-\infty}^{+\infty}\int_{-\infty}^{+\infty} \omega\sqrt{\xi^2-\omega^2}\,|\hat{\phi}(\xi,\omega)|^2 d\omega d\xi \\ &= \frac{1}{2}\int_{-\infty}^{+\infty}\int_{|\omega|\geq|\xi|} |\omega|\sqrt{\omega^2-\xi^2}\,|\hat{\phi}(\xi,\omega)|^2 d\omega d\xi \end{aligned} \tag{2.30}$$

where in the last equality we have used (2.29) and the symmetry $|\widehat{\phi_t}(\xi,\omega)| = |\widehat{\phi_t}(\xi,-\omega)|$ (recall that ϕ is real-valued).
In the case when $\phi(\cdot,T)$ does not vanish the localization to the interval $[0,T]$ is a bit harder and a positive extra term must be added to (2.30). In fact, we need the following

Proposition 2.1. *The quadratic form $a_{\mathscr{E}}(\phi,\phi)$ is defined in the space of functions $H^1([0,T];H^{1/2}_{00}(\Gamma))$, vanishing for $t=0$, and we have*

$$\begin{aligned} a_{\mathscr{E}}(\phi,\phi) &= \frac{1}{2}\int_{-\infty}^{+\infty}\int_{\{|\omega|\geq|\xi|\}} \frac{\sqrt{\omega^2-\xi^2}}{|\omega|}\,|\widehat{\phi}_t(\xi,\omega)|^2 d\omega d\xi \\ &+ \frac{1}{4}\int_{-\infty}^{+\infty}|\xi|\,|\tilde{\phi}(\xi,T)|^2 d\xi. \end{aligned} \tag{2.31}$$

In (2.31), the meaning of $\widehat{\phi}_t(\xi,\omega)$ is the following

$$\widehat{\phi}_t(\xi,\omega) = \frac{1}{2\pi}\int_0^L\int_0^T e^{-i(x\xi+t\omega)}\,\phi_t(x,t)\,dt\,dx. \tag{2.32}$$

Proof. We provide only a sketch of the proof. Let us extend $\phi\in H^1([0,T];H^{1/2}_{00}(\Gamma))$ to the whole time axis, by setting $\Phi(x,t)=\phi(x,T)$ for $t>T$, and $\Phi(x,t)=0$ for $t<0$. Since $\phi(\cdot,0)=0$, it not difficult to see that $\Phi\in\mathscr{H}_\sigma$ for every $\sigma>0$. Then we are allowed to apply formula (2.27), for $\phi=\psi=\Phi$. Since $\Phi_t(x,t)=0$ for $t>T$, we get, ($z=\omega-i\sigma$, $\sigma>0$)

$$\begin{aligned} &\int_0^L\int_0^T e^{-2\sigma t}(D\phi)(x,t)\phi_t(x,t)dtdx = \int_0^L\int_0^{+\infty} e^{-2\sigma t}(D\Phi)(x,t)\Phi_t(x,t)dtdx \\ &= \frac{1}{2}\int_{-\infty}^{+\infty}\int_{-\infty}^{+\infty}\sqrt{\xi^2-z^2}\,\widehat{\Phi}(\xi,z)\overline{\widehat{\Phi_t}(\xi,z)}d\omega d\xi. \end{aligned}$$

Owing to the identity $iz\widehat{\Phi}(\xi,z)=\widehat{\Phi_t}(\xi,z)$ and since $\widehat{\Phi_t}(\xi,z)=\widehat{\phi}_t(\xi,z)$, we have also

$$\begin{aligned} &\int_0^L\int_0^T e^{-2\sigma t}(D\phi)(x,t)\phi_t(x,t)dtdx = \frac{1}{2}\int_{-\infty}^{+\infty}\int_{-\infty}^{+\infty}\frac{\sqrt{\xi^2-z^2}}{iz}\,|\widehat{\Phi_t}(\xi,z)|^2\,d\omega d\xi \\ &= \frac{1}{2}\int_{-\infty}^{+\infty}\int_{-\infty}^{+\infty}\frac{\sqrt{\xi^2-z^2}}{iz}\,|\widehat{\phi}_t(\xi,z)|^2\,d\omega d\xi. \end{aligned} \tag{2.33}$$

Of course, the main difficulty in passing to the limit $\sigma\to 0^+$ in formula (2.33), is due to the singularity $1/z=1/(\omega-i\sigma)$ in the right-hand integral. To overcome this difficulty one may argue as in the proof of the distributional limit (here *p.v.* stands for Cauchy principal value)

$$\lim_{\sigma\to 0^+}\frac{1}{\omega-i\sigma} = p.v.\left(\frac{1}{\omega}\right)+\pi\,\delta(\omega).$$

First we split the integral (2.33) in two parts:

$$\frac{1}{2}\int_{-\infty}^{+\infty}\int_{-\infty}^{+\infty}\frac{\sqrt{\xi^2-z^2}}{iz}\,|\widehat{\phi}_t(\xi,z)|^2\,d\omega d\xi = \frac{1}{2}\int_{-\infty}^{+\infty}\int_{|\omega|\geq\varepsilon}\cdots+\frac{1}{2}\int_{-\infty}^{+\infty}\int_{|\omega|<\varepsilon}\cdots$$

By applying Lebesgue's dominated convergence Theorem, one gets

$$\lim_{\sigma\to 0^+}\frac{1}{2}\int_{-\infty}^{+\infty}\int_{|\omega|\geq\varepsilon}\frac{\sqrt{\xi^2-z^2}}{iz}|\widehat{\phi}_t(\xi,z)|^2\,d\omega d\xi=\frac{1}{2}\int_{-\infty}^{+\infty}\int_{|\omega|\geq\varepsilon}\frac{\sqrt{\xi^2-\omega^2}}{i\omega}|\widehat{\phi}_t(\xi,\omega)|^2\,d\omega d\xi.$$

The passage to the limit as $\varepsilon\to 0^+$ gives rise to

$$p.v.\frac{1}{2}\int_{-\infty}^{+\infty}\int_{-\infty}^{+\infty}\frac{\sqrt{\xi^2-\omega^2}}{i\omega}|\widehat{\phi}_t(\xi,\omega)|^2\,d\omega\,d\xi=\frac{1}{2}\int_{-\infty}^{\infty}d\xi\int_{|\omega|\geq|\xi|}\frac{\sqrt{\omega^2-\xi^2}}{|\omega|}|\widehat{\phi}_t(\xi,\omega)|^2\,d\omega$$

where we have used the determination of the square root (2.29) and the symmetry $|\widehat{\phi}_t(\xi,\omega)|=|\widehat{\phi}_t(\xi,-\omega)|$. The double limit in the second term (the $\delta(\omega)$ term) is a bit harder to treat but can be justified with an argument similar to those used in paper [Lebeau and Schatzman (1984)]. Formally, one gets

$$\frac{\pi}{2}\int_{-\infty}^{+\infty}\delta(\omega)d\omega\int_{-\infty}^{+\infty}\sqrt{\xi^2-\omega^2}\,|\widehat{\phi}_t(\xi,\omega)|^2\,d\xi=\frac{\pi}{2}\int_{-\infty}^{+\infty}|\xi|\,|\widehat{\phi}_t(\xi,0)|^2\,d\xi.$$

On the other hand for $\omega=0$, we have

$$\widehat{\phi}_t(\xi,0)=\frac{1}{\sqrt{2\pi}}\int_0^T\widetilde{\phi}_t(\xi,t)dt=\frac{1}{\sqrt{2\pi}}\widetilde{\phi}(\xi,T)$$

since $\widetilde{\phi}(\xi,0)=\frac{1}{\sqrt{2\pi}}\int_0^L e^{-ix\xi}\phi(x,0)dx=0$. It follows that

$$\frac{\pi}{2}\int_{-\infty}^{+\infty}|\xi|\,|\widehat{\phi}_t(\xi,0)|^2\,d\xi=\frac{1}{4}\int_{-\infty}^{+\infty}|\xi|\,|\widetilde{\phi}(\xi,T)|^2\,d\xi.$$

■

We remark that in the case $\phi\in H_0^1([0,T];H_{00}^{1/2}(\Gamma))$ formulae (2.31) and (2.30) agree since $\widehat{\phi}_t(\xi,\omega)=i\omega\widehat{\phi}(\xi,\omega)$ and $\widetilde{\phi}(\xi,T)=0$.

Now we come to the main question of this section: the coerciveness properties of the energy functional. Two simple considerations can be drawn by the fact that the domain of integration in formula (2.31) is the cone $\mathscr{C}:=\{(\xi,\omega):|\omega|>|\xi|\}$. The first one is that the energy is a strictly positive functional. This follows immediately from the fact that, owing to the Paley-Wiener Theorem, $\widehat{\phi}_t$ as defined in (2.32) is an entire analytic function. Therefore it cannot vanish in $\mathscr{C}$ unless it vanishes on the whole $\mathbb{R}^2$. The second and more relevant consideration is that most of the information regarding oscillations in the space variable is not taken into account by the energy. This remark is made more precise by the fact that the quadratic form

$a_{\mathscr{E}}(\phi,\phi)$ cannot be coercive with respect to any Sobolev norm. The proof of this assertion is very similar to the case of the single layer operator, which has been given in full details in [Aimi, Diligenti, Guardasoni, Mazzieri and Panizzi (2009)].

A first weak coerciveness property for $a_{\mathscr{E}}(\phi,\phi)$ can be obtained by the following considerations. Let us fix $P>0$ and consider the following maximum problem:

$$\lambda_0 = \max\left\{\int_{-P}^{P} |\hat{f}(\omega)|^2\,d\omega : f\in L^2(0,T),\ \int_0^T |f(t)|^2\,dt = 1\right\}. \tag{2.34}$$

It is not difficult to see that the following properties hold true: $\lambda_0 = \lambda_0(TP) < 1$, $\lambda_0(\rho)$ is an increasing function and that $\lim_{\rho\to 0^+}\lambda_0(\rho)=0$, $\lim_{\rho\to+\infty}\lambda_0(\rho)=1$. The number $\lambda_0(TP)$ is the first eigenvalue of the so called time-band limited operator which has been deeply studied in the sixties by Slepian, Landau and Pollack (see e.g. [Slepian (1983)]). Let us fix ξ and set $P=|\xi|$, $f=\widehat{\phi_t}(\xi,\cdot)$. From (2.31), we get

$$\begin{aligned} a_{\mathscr{E}}(\phi,\phi) &\geq \frac{1}{2\sqrt{2}}\int_{-\infty}^{+\infty} d\xi \int_{|\omega|>\sqrt{2}|\xi|} |\widehat{\phi_t}(\xi,\omega)|^2\,d\omega \\ &\geq \frac{1}{2\sqrt{2}}\int_{-\infty}^{+\infty} d\xi \int_{-\infty}^{+\infty} (1-\lambda_0(\sqrt{2}|\xi|T))\,|\widehat{\phi_t}(\xi,\omega)|^2\,d\omega. \end{aligned}$$

Unfortunately, when $\rho\to+\infty$, the function $1-\lambda_0(\rho)$ tends to zero exponentially. More precisely, Fuchs in [Fuchs (1964)] has shown that

$$1-\lambda_0(\rho) \sim 2\sqrt{2\pi\rho}\,e^{-\rho}, \qquad \rho\to+\infty.$$

Therefore, by the properties of $\lambda_0(\rho)$, we can only conclude that there exists a constant $C>0$ such that

$$1-\lambda_0(\rho) \geq C\sqrt{1+\rho}\,e^{-\rho} \qquad (\rho>0).$$

As a consequence, we obtain the following estimate

$$a_{\mathscr{E}}(\phi,\phi) \geq C\int_{-\infty}^{+\infty} d\xi \int_{-\infty}^{+\infty} \sqrt{1+\sqrt{2}|\xi|T}\,e^{-\sqrt{2}|\xi|T}|\widehat{\phi_t}(\xi,\omega)|^2\,d\omega.$$

Other more interesting coerciveness properties can be obtained by restricting the quadratic form $a_{\mathscr{E}}(\cdot,\cdot)$ to suitable infinite-dimensional subspaces of $H^1((0,T);H_{00}^{1/2}(\Gamma))$, for instance by fixing the space step Δx for the mesh on the crack Γ and letting the time step Δt tend to zero. More precisely, let $n\geq 1$ be a fixed integer, set $\Delta x = L/n$ and consider the functions

$$v(x,t) = \sum_{k=0}^{n-1} f_k(t)\,\psi_k(x).$$

Here $\psi_k(x) = \psi(x/\Delta x - k\Delta x)$, $k = 0,...,n-1$ and $\psi(x) = (1-|x|)H(1-|x|)$ is the usual hat function. The functions $f_k(t)$, $k = 0,...,n-1$, are in $H^1(0,T)$ and vanish for $t = 0$. We denote by $\mathscr{V}_n$ the infinite-dimensional space of such functions and remark that $\mathscr{V}_n \subset H^1((0,T);H^{1/2}_{00}(\Gamma))$.

Theorem 2.1. *For any $v \in \mathscr{V}_n$ we have*

$$a_{\mathscr{E}}(v,v) \geq \frac{8\Delta x}{\sqrt{2}\pi^4}\left[1-\lambda_0(\sqrt{2}\pi T/\Delta x)\right]\|v_t\|^2_{L^2((0,T);L^2(\Gamma))} \tag{2.35}$$

where λ_0 is defined in (2.34).

Proof. By computing the Fourier transform of v_t, we get

$$\widehat{v_t}(\xi,\omega) = \sqrt{\frac{2}{\pi}}\,\Delta x\,\frac{1-\cos(\Delta x\xi)}{(\Delta x\xi)^2}\sum_{k=1}^{n-1} e^{-ik\Delta x\xi}\,\widehat{f_{kt}}(\omega).$$

Let us set $G(\Delta x\xi) := \dfrac{1-\cos(\Delta x\xi)}{(\Delta x\xi)^2}$. From (2.31), we have

$$\begin{aligned}
a_{\mathscr{E}}(v,v) &\geq \frac{(\Delta x)^2}{\pi}\int_{-\infty}^{+\infty}\int_{\{|\omega|>|\xi|\}} G^2(\Delta x\xi)\frac{\sqrt{\omega^2-\xi^2}}{|\omega|}\left|\sum_{k=1}^{n-1} e^{-ik\Delta x\xi}\,\widehat{f_{kt}}(\omega)\right|^2 d\xi\,d\omega \\
&\geq \frac{(\Delta x)^2}{\sqrt{2}\pi}\int_{-\infty}^{+\infty}\int_{\{|\omega|>\sqrt{2}|\xi|\}} G^2(\Delta x\xi)\left|\sum_{k=1}^{n-1} e^{-ik\Delta x\xi}\,\widehat{f_{kt}}(\omega)\right|^2 d\xi\,d\omega \\
&= \frac{\Delta x}{\sqrt{2}\pi}\int_{-\infty}^{+\infty} d\omega\int_{|\xi|\leq\frac{\Delta x|\omega|}{\sqrt{2}}} G^2(\xi)\left|\sum_{k=1}^{n-1} e^{-ik\xi}\,\widehat{f_{kt}}(\omega)\right|^2 d\xi \\
&\geq \frac{\Delta x}{\sqrt{2}\pi}\int_{|\omega|\geq\frac{\pi\sqrt{2}}{\Delta x}} d\omega\int_{|\xi|\leq\frac{\Delta x|\omega|}{\sqrt{2}}} G^2(\xi)\left|\sum_{k=1}^{n-1} e^{-ik\xi}\,\widehat{f_{kt}}(\omega)\right|^2 d\xi \\
&\geq \frac{4\Delta x}{\sqrt{2}\pi^5}\int_{|\omega|\geq\frac{\pi\sqrt{2}}{\Delta x}} d\omega\int_{-\pi}^{\pi}\left|\sum_{k=1}^{n-1} e^{-ik\xi}\,\widehat{f_{kt}}(\omega)\right|^2 d\xi
\end{aligned}$$

where in the last inequality we have used that $G(\xi) \geq 2/\pi^2$ for $|\xi| \leq \pi$. On the other hand, we have for every ω,

$$\int_{-\pi}^{\pi}\left|\sum_{k=1}^{n-1} e^{-ik\xi}\,\widehat{f_{kt}}(\omega)\right|^2 d\xi = 2\pi\sum_{k=1}^{n-1}|\widehat{f_{kt}}(\omega)|^2.$$

It follows that

$$a_{\mathscr{E}}(v,v) \geq \frac{8\Delta x}{\sqrt{2}\pi^4} \sum_{k=1}^{n-1} \int_{|\omega|\geq(\pi\sqrt{2})/\Delta x} |\widehat{f_{kt}}(\omega)|^2 \, d\omega.$$

By definition of λ_0 and Parseval identity, we get

$$\begin{aligned} a_{\mathscr{E}}(v,v) &\geq \frac{8\Delta x}{\sqrt{2}\pi^4} \left[1-\lambda_0(\sqrt{2}\pi T/\Delta x)\right] \sum_{k=1}^{n-1} \int_{-\infty}^{+\infty} |\widehat{f_{kt}}(\omega)|^2 \, d\omega \\ &= \frac{8\Delta x}{\sqrt{2}\pi^4} \left[1-\lambda_0(\sqrt{2}\pi T/\Delta x)\right] \sum_{k=1}^{n-1} \int_0^T |f_k'(t)|^2 \, dt. \end{aligned}$$

The assertion follows since, from a simple computation, we have

$$\|v_t\|^2_{L^2((0,T);L^2(\Gamma))} = \int_0^L \int_0^T \left| \sum_{k=0}^{n-1} f_k'(t)\, \psi_k(x) \right|^2 dt\, dx \leq \Delta x \sum_{k=1}^{n-1} \int_0^T |f_k'(t)|^2 \, dt.$$

■

Remark 1. Since $v(x,0)=0$, $\|v_t\|_{L^2((0,T);L^2(\Gamma))}$ is an equivalent $H^1([0,T];\, L^2(\Gamma))$ norm. In particular we have $\|v\|_{L^2((0,T);\, L^2(\Gamma))} \leq T\, \|v_t\|_{L^2((0,T);\, L^2(\Gamma))}$. Therefore, (2.35) can be written also with respect to $\|v\|^2_{L^2((0,T);\, L^2(\Gamma))}$ with a T^{-2} extra factor (see Tab. 2 in Section 4 for the related numerical tests).

Remark 2. It's reasonable to expect that the obtained theoretical results still hold for more general geometries of the open arc Γ, or even in the case when the obstacle is a convex domain in $\mathbb{R}^2$.

Remark 3. In the past years and in different contexts, several authors [Ha Duong (1990); Lebeau and Schatzman (1984); Miyatake (1993)] have dealt with the properties of the Dirichlet - Neumann operator

$$D:\ [u] \longmapsto \frac{\partial u}{\partial n} \qquad (x,t) \in \Gamma \times (0,+\infty), \tag{2.36}$$

related to the wave equation in the case of a flat boundary Γ. In [Lebeau and Schatzman (1984)] the authors study the positivity properties of the quadratic form $< D\phi, \phi >$. In reference [Ha Duong (1990)], devoted to the transient BIE for the acoustic equation, Ha Duong performs a detailed analysis of the operator (2.36) by recurring to the Fourier-Laplace transform with non vanishing imaginary part σ in the phase variable $\omega - i\sigma$. Under the restriction $\sigma \geq \sigma_0 > 0$, in [Ha Duong (1990)] optimal results are obtained in terms of regularity and stability of the associated bilinear form. As shown in the same paper, it is possible to obtain coerciveness passing to the limit $\sigma \to 0^+$, if instead of $\mathscr{E}(T,u)$, one considers the functional

$$\int_0^T \mathscr{E}(t,u)\,dt.$$

3 Galerkin BEM discretization

We consider for a crack Γ of length L, a boundary mesh constituted by M straight elements $\{e_1,\cdots,e_M\}$, with $length(e_i) \leq \Delta x$, $e_i \cap e_j = \emptyset$ if $i \neq j$ and such that $\bigcup_{i=1}^M \overline{e}_i$ coincides with $\overline{\Gamma}$ if the crack is (piece-wise) linear, or is a suitable approximation of $\overline{\Gamma}$, otherwise. The functional background compels one to choose spatially shape functions belonging to $H_0^1(\Gamma)$ for our Neumann problems. Hence we use standard piece-wise polynomial boundary element functions $w_j(\mathbf{x})$, $j = 1,\cdots,M_{\Delta x}$, suitably defined in relation to the introduced mesh over Γ.
For time discretization we consider a uniform decomposition of the time interval $[0,T]$ with time step $\Delta t = T/N_{\Delta t}$,$N_{\Delta t} \in \mathbb{N}^+$, generated by the $N_{\Delta t}+1$ instants

$$t_k = k\Delta t, \quad k = 0,\cdots,N_{\Delta t}$$

and we choose temporally piece-wise linear shape functions, although higher degree shape functions can be used. Note that, for this particular choice, shape functions, denoted with $v_k(t)$, $k = 0,\cdots,N_{\Delta t}-1$, will be defined as

$$v_k(t) = R(t-t_k) - 2R(t-t_{k+1}) + R(t-t_{k+2}),$$

where $R(t-t_k) = \frac{t-t_k}{\Delta t} H[t-t_k]$ is the ramp function, and they will give contribution to the second time derivative in (2.8) in terms of Dirac distributions. Hence, the unknown approximate solution of the problem at hand will be expressed as

$$\sum_{k=0}^{N_{\Delta t}-1} \sum_{j=1}^{M_{\Delta x}} \alpha_j^{(k)} w_j(\mathbf{x})\, v_k(t). \tag{3.37}$$

The Galerkin BEM discretization coming from energetic weak formulation produces the linear system

$$A_{\mathscr{E}}\, x_{\mathscr{E}} = b_{\mathscr{E}}. \tag{3.38}$$

Having set $\Delta_{hk} = t_h - t_k$, matrix elements, after a double analytic integration in the time variables, are of the form

$$\sum_{\alpha,\beta,\delta=0}^{1} (-1)^{\alpha+\beta+\delta} \int_\Gamma w_i(\mathbf{x}) \int_\Gamma H[\Delta_{h+\alpha\, k+\beta+\delta} - r]\, \mathscr{D}(r, t_{h+\alpha}, t_{k+\beta+\delta})\, w_j(\boldsymbol{\xi})\, d\gamma_{\boldsymbol{\xi}}\, d\gamma_{\mathbf{x}},$$

(3.39)

where

$$\begin{aligned}\mathscr{D}(r,t_h,t_k) &= \frac{1}{2\pi\Delta t^2}\left\{\frac{\mathbf{r}\cdot\mathbf{n_x}\ \mathbf{r}\cdot\mathbf{n_\xi}}{r^2}\ \frac{\Delta_{hk}\sqrt{\Delta_{hk}^2-r^2}}{r^2}+\right.\\ &\left.\frac{(\mathbf{n_x}\cdot\mathbf{n_\xi})}{2}\left[\log(\Delta_{hk}+\sqrt{\Delta_{hk}^2-r^2})-\log r-\frac{\Delta_{hk}\sqrt{\Delta_{hk}^2-r^2}}{r^2}\right]\right\}.\end{aligned} \tag{3.40}$$

Anyway, the above elements depend on the difference t_h-t_k and in particular they vanish if $t_h \le t_k$. Hence, matrix $A_{\mathscr{E}}$ has a block lower triangular Toeplitz structure. Each block has dimension $M_{\Delta x}$. If we indicate with $A_{\mathscr{E}}^{(\ell)}$ the block obtained when $t_h-t_k=(\ell+1)\Delta t$, $\ell=0,\ldots,N_{\Delta t}-1$, the linear system can be written as

$$\begin{pmatrix} A_{\mathscr{E}}^{(0)} & 0 & 0 & \cdots & 0\\ A_{\mathscr{E}}^{(1)} & A_{\mathscr{E}}^{(0)} & 0 & \cdots & 0\\ A_{\mathscr{E}}^{(2)} & A_{\mathscr{E}}^{(1)} & A_{\mathscr{E}}^{(0)} & \cdots & 0\\ \cdots & \cdots & \cdots & \cdots & 0\\ A_{\mathscr{E}}^{(N_{\Delta t}-1)} & A_{\mathscr{E}}^{(N_{\Delta t}-2)} & \cdots & A_{\mathscr{E}}^{(1)} & A_{\mathscr{E}}^{(0)}\end{pmatrix}\begin{pmatrix}\alpha^{(0)}\\ \alpha^{(1)}\\ \alpha^{(2)}\\ \vdots\\ \alpha^{(N_{\Delta t}-1)}\end{pmatrix}=\begin{pmatrix} b_{\mathscr{E}}^{(0)}\\ b_{\mathscr{E}}^{(1)}\\ b_{\mathscr{E}}^{(2)}\\ \vdots\\ b_{\mathscr{E}}^{(N_{\Delta t}-1)}\end{pmatrix} \tag{3.41}$$

where

$$\alpha^{(\ell)}=\left(\alpha_j^{(\ell)}\right) \quad \text{and} \quad b_{\mathscr{E}}^{(\ell)}=\left(b_{\mathscr{E},j}^{(\ell)}\right), \quad \text{with} \quad \ell=0,\ldots,N_{\Delta t}-1;\ j=1,\ldots,M_{\Delta x}. \tag{3.42}$$

The solution of (3.41) is obtained with a block forward substitution, i.e. at every time instant $t_\ell=(\ell+1)\Delta t$, $\ell=0,\cdots,N_{\Delta t}-1$, we solve a reduced linear system of the type:

$$A_{\mathscr{E}}^{(0)}\alpha^{(\ell)}=b_{\mathscr{E}}^{(\ell)}-(A_{\mathscr{E}}^{(1)}\alpha^{(\ell-1)}+\cdots+A_{\mathscr{E}}^{(\ell)}\alpha^{(0)}). \tag{3.43}$$

Procedure (3.43) is a time-marching technique, where the only matrix to be inverted is the positive definite $A_{\mathscr{E}}^{(0)}$ diagonal block, while all the other blocks are used to update at every time step the right-hand side. Owing to this procedure we can construct and store only the blocks $A_{\mathscr{E}}^{(0)},\cdots,A_{\mathscr{E}}^{(N_{\Delta t}-1)}$ with a considerable reduction of computational cost and memory requirement.

Further, the energetic matrix $A_{\mathscr{E}}$ has an interesting property: for a fixed space discretization Δx and for vanishing Δt, blocks $\Delta t A_{\mathscr{E}}^{(0)}$ tend to the mass matrix $M^{(0)}$ of order $M_{\Delta x}$, with elements

$$M_{ij}^{(0)} = \frac{1}{2}\int_{\Gamma} w_i(\mathbf{x})\, w_j(\mathbf{x})\, d\gamma_{\mathbf{x}}, \tag{3.44}$$

blocks $\Delta t A_{\mathscr{E}}^{(1)}$ tend to $-M^{(0)}$ and blocks $\Delta t A_{\mathscr{E}}^{(\ell)}$, $\ell = 2,\ldots,N_{\Delta t}-1$ tend to the zero matrix of order $M_{\Delta x}$. Hence $\Delta t A_{\mathscr{E}}$ tends to a limit matrix which has the following lower block bidiagonal structure, with $N_{\Delta t}$ blocks:

$$\begin{pmatrix} M^{(0)} & 0 & 0 & 0 & \cdots & 0 \\ -M^{(0)} & M^{(0)} & 0 & 0 & \cdots & 0 \\ 0 & -M^{(0)} & M^{(0)} & 0 & \cdots & 0 \\ 0 & 0 & -M^{(0)} & M^{(0)} & \cdots & 0 \\ \cdots & \cdots & \cdots & \cdots & \cdots & 0 \\ 0 & 0 & \cdots & 0 & -M^{(0)} & M^{(0)} \end{pmatrix}. \tag{3.45}$$

Let us prove this result for the case of a straight crack of length L. Having set $r = |x-\xi|$, the generic element of the block $\Delta t A_{\mathscr{E}}^{(0)}$ is of the form

$$\begin{aligned} &\Delta t \int_0^L w_i(x) \int_0^L H[\Delta t - r]\mathscr{D}(r,t_1,t_0)\, w_j(\xi)\, d\xi\, dx \\ &= \frac{1}{4\pi\Delta t}\int_0^L w_i(x)\int_0^L H[\Delta t - r]\Big[\log\big(\frac{\Delta t + \sqrt{\Delta t^2 - r^2}}{r}\big) - \frac{\Delta t\sqrt{\Delta t^2-r^2}}{r^2}\Big]\, w_j(\xi)\, d\xi\, dx \\ &= \frac{1}{4\pi\Delta t}\int_0^L w_i(x) \\ &\int_{[0,L]\cap\{\frac{r}{\Delta t}<1\}} \Big[\log\Big(\frac{1+\sqrt{1-\left(\frac{r}{\Delta t}\right)^2}}{\frac{r}{\Delta t}}\Big) - \Big(\frac{r}{\Delta t}\Big)^{-2}\sqrt{1-\Big(\frac{r}{\Delta t}\Big)^2}\Big]\, w_j(\xi)\, d\xi\, dx. \end{aligned}$$

Now, with the change of variable in the inner integration $\eta = \frac{\xi - x}{\Delta t}$, we obtain

$$\frac{1}{4\pi}\int_0^L w_i(x)\int_{\max\{-1,\frac{-x}{\Delta t}\}}^{\min\{1,\frac{L-x}{\Delta t}\}} \Big[\log\Big(\frac{1+\sqrt{1-\eta^2}}{|\eta|}\Big) - \eta^{-2}\sqrt{1-\eta^2}\Big]\, w_j(x+\eta\,\Delta t)\, d\eta\, dx.$$

For vanishing Δt, the above integral can be rewritten as

$$\frac{1}{4\pi}\int_0^L w_i(x)w_j(x)\int_{-1}^{1} \Big[\log\Big(\frac{1+\sqrt{1-\eta^2}}{|\eta|}\Big) - \eta^{-2}\sqrt{1-\eta^2}\Big]\, d\eta\, dx$$

and evaluating analytically the hypersingular inner integral in the Hadamard Finite Part sense, one finally gets (3.44).
For the other blocks $\Delta t A_{\mathscr{E}}^{(\ell)}$, $\ell = 1, \cdots, N_{\Delta t} - 1$ one can proceed in the same way, obtaining the whole limit matrix (3.45).

For what concerns the effective evaluation of the elements of matrix $A_{\mathscr{E}}$, in the sequel, we will refer to one of the double integrals in (3.39), indicated by

$$\int_\Gamma w_i(\mathbf{x}) \int_\Gamma H[\Delta_{hk} - r]\, \mathscr{D}(r, t_h, t_k)\, w_j(\boldsymbol{\xi})\, d\gamma_{\boldsymbol{\xi}}\, d\gamma_{\mathbf{x}}. \tag{3.46}$$

Using the standard element by element technique, the evaluation of every double integral of the form (3.46) is reduced to the assembling of local contributions of the type

$$\int_{e_i} \widetilde{w}_i^{(d_i)}(\mathbf{x}) \int_{e_j} H[\Delta_{hk} - r]\, \mathscr{D}(r, t_h, t_k)\, \widetilde{w}_j^{(d_j)}(\boldsymbol{\xi})\, d\gamma_{\boldsymbol{\xi}}\, d\gamma_{\mathbf{x}}, \tag{3.47}$$

where $\widetilde{w}_i^{(d_i)}$, $\widetilde{w}_j^{(d_j)}$ define one of the local lagrangian basis function in the space variable of degree d_i, d_j defined over the elements e_i, e_j of the boundary mesh, respectively.
Looking at (3.40), we observe space singularities of type $\log r$ and $O(r^{-2})$ as $r \to 0$, which are typical of weakly singular and hypersingular kernels related to two-dimensional elliptic problems. Hence, efficient evaluation of double integrals of type (3.47) is particularly required when $e_i \equiv e_j$ and when e_i, e_j are consecutive. Note that when the kernel is hypersingular and $e_i \equiv e_j$ we have to define both the inner and the outer integrals as Hadamard finite parts, while if e_i and e_j are consecutive, only the outer integral must be understood in the finite part sense: the correct interpretation of double integrals is the key point for any efficient numerical approach based on element by element technique (see [Aimi, Diligenti and Monegato (1997)]). Further, we observe that the Heaviside function $H[\Delta_{hk} - r]$ in (3.47) and the function $\sqrt{\Delta_{hk}^2 - r^2}$ in the kernel $\mathscr{D}(r, t_h, t_k)$, give rise to other different type of troubles, which have to be properly faced, as described in [Aimi, Diligenti and Guardasoni (2009)]. Hence, the numerical treatment of (3.47) has been operated through quadrature schemes widely used in the context of Galerkin BEM coming from elliptic problems [Aimi, Diligenti and Monegato (1997)], coupled with a suitable regularization technique [Monegato and Scuderi (1999)], after a careful subdivision of the integration domain due to the presence of the Heaviside function. A detailed illustration of the efficient numerical integrations employed for the discretization of hypersingular BIEs related to wave propagation problems and which represent a valid alternative to those proposed in [Gallego and Dominguez (1996); Zhang (2002)], can be found in [Aimi, Diligenti and Guardasoni (2010)].

4 Numerical results

In this section, we present several of numerical results related to two-dimensional Neumann exterior problem (2.1)-(2.3): some of them can be found also in [Aimi, Diligenti, Guardasoni, Mazzieri and Panizzi (2009)], but they have been reported here for the sake of completeness and with a deeper numerical study. In fact, the first part of examples is devoted to a numerical analysis of the obtained results, while the aim of the second part is to give a qualitative analysis of the simulations. We start with the rectilinear obstacle $\Gamma = \{(x,0) : x \in [0,1]\}$. The incident wave $u^I(\mathbf{x},t)$ is a plane wave propagating in direction $\mathbf{k}$ with unitary amplitude:

$$u^I(\mathbf{x},t) = f(t - \mathbf{k}\cdot\mathbf{x}), \quad \text{with} \quad \mathbf{k} = (\cos\theta, \sin\theta). \tag{4.48}$$

Hence, the Neumann datum on Γ in (2.3) will be:

$$g(x,t) = -\frac{\partial}{\partial \mathbf{n_x}} f(t - \mathbf{k}\cdot\mathbf{x})\Big|_{\Gamma}. \tag{4.49}$$

We show the results obtained for two different functions, that have been chosen for the known asymptotic behavior of the solution, which allows us to validate the approximate solution, in the sequel indicated with $\phi(x,t)$.

Plane linear wave. The first example is taken from [Becache (1993)], where the Neumann boundary conditions comes from this choice of f:

$$f(t) = tH[t].$$

In this case, the Neumann datum (4.49) tends to the constant value $g_\theta = \sin\theta$ when t tends to infinity. The solution u tends to the solution of the static problem

$$\begin{cases} -\triangle u_\infty = 0 \quad \text{in} \quad \mathbb{R}^2 \setminus \Gamma, \quad u(\mathbf{x}) = O(\|\mathbf{x}\|_2^{-1}) \quad \text{for} \quad \|\mathbf{x}\|_2 \to \infty \\ \dfrac{\partial u_\infty}{\partial \mathbf{n}} = g_\theta \quad \text{on} \quad \Gamma \end{cases} \tag{4.50}$$

and the associated jump $\phi_\theta^\infty(x) = [u_\infty]$ across Γ can be computed explicitly:

$$\phi_\theta^\infty(x) = \sin\theta\sqrt{x(1-x)}.$$

Hence, we can compare the solution $\phi(x,t)$ with the static solution $\phi_\theta^\infty(x)$.

The crack Γ has been uniformly decomposed with discretization parameters $\Delta x = 0.1, 0.05, 0.025$ and equipped with spatial linear shape and test functions; the observation time interval $[0,T] = [0,10]$ has been uniformly subdivided with time steps $\Delta t = 0.05, 0.025$. In Fig. 1, we present the numerical solution obtained for large times in some points of Γ, for $\theta = \frac{\pi}{3}$, $\Delta x = 0.05$ and $\Delta t = 0.025$: it appears in

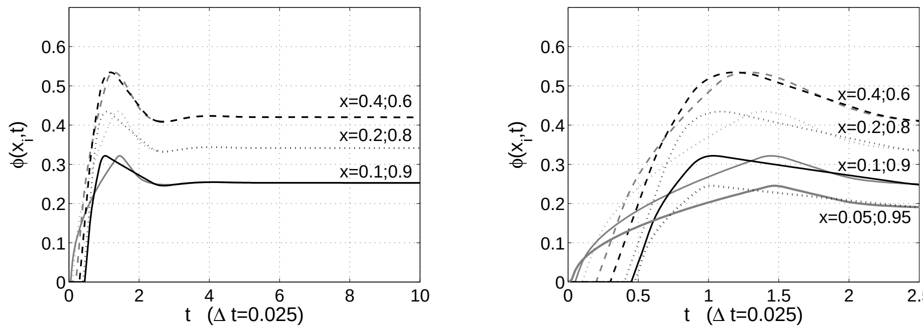

Figure 1: Density $\phi(x,t)$ evaluated in some points of Γ for $\theta = \pi/3$.

perfect agreement with the corresponding one reported in [Becache (1993)]. Note that points of Γ, symmetric with respect to $x = 0.5$ behaves in different ways at the beginning of the simulation, since the incident wave does not strike simultaneously the crack; then they assume a symmetric behavior for sufficiently large times. Further, to show that the whole numerical solution $\phi(x,t)$ stabilizes itself, we report in Fig. 2 the COD on Γ in different time instants $t \geq 4$.

To better specify this issue, in Fig. 3, we show the graph of time functions

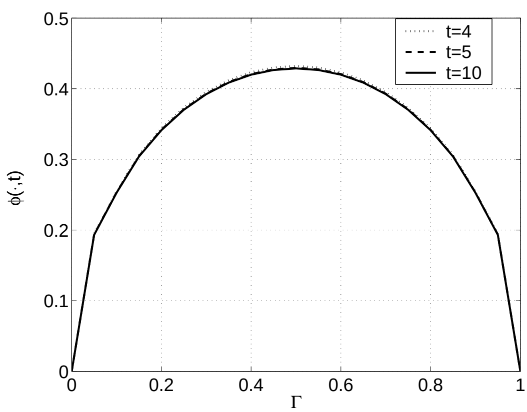

Figure 2: Solution $\phi(x,t)$ in different time instants, for $\theta = \pi/3$.

$\|\phi(\cdot,t) - \phi_\theta^\infty(\cdot)\|_{L^1(\Gamma)}$ evaluated for different parameters Δx, having fixed $\Delta t = 0.05$. As one can observe, for large times the transient numerical solution stabilizes itself producing an error, w.r.t. the analytical static solution, which decreases linearly w.r.t. Δx. This feature is evident in Tab. 1, where $|\phi(x,t) - \phi_\theta^\infty(x)|$

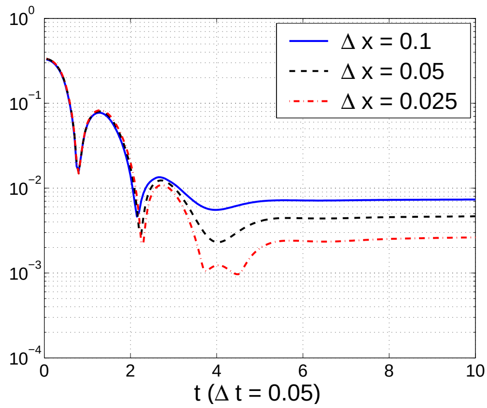

Figure 3: Time function $\|\phi(\cdot,t) - \phi_\theta^\infty(\cdot)\|_{L^1(\Gamma)}$ evaluated for some parameters Δx, for $\theta = \pi/3$.

has been evaluated in some nodes of the crack and in different time instants, for $\Delta x = 0.1, 0.05, 0.025$ and $\Delta t = 0.05$.

In Fig. 4, we show numerical results obtained for $\theta = \frac{\pi}{4}$, $\Delta x = 0.05$, $\Delta t = 0.025$, analogous to those in Fig. 1, and in Fig. 5 we present the approximate COD for $T = 4, 5, 10$ together with the analytical solution of the corresponding static problem: the four curves overlap each other. Similar figures have been obtained varying

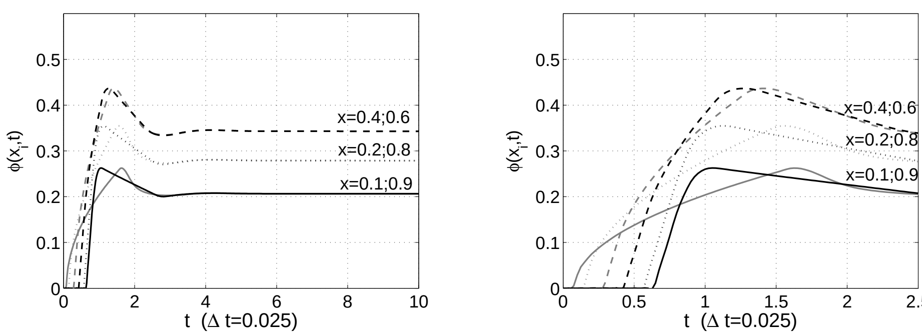

Figure 4: Density $\phi(x,t)$ evaluated in some points of Γ for $\theta = \pi/4$.

discretization parameters $\Delta t, \Delta x$. In any case, numerical results appear in agreement with those reported in [Becache (1993)], but differently from what is said in that paper, they are stable regardless of the ratio $\frac{\Delta t}{\Delta x}$.

$\Delta x = 0.1$					
	$t = 6$	$t = 7$	$t = 8$	$t = 9$	$t = 10$
$x = 0.1$	$6.4351\,10^{-3}$	$6.4059\,10^{-3}$	$6.3017\,10^{-3}$	$6.2505\,10^{-3}$	$6.2128\,10^{-3}$
$x = 0.2$	$1.0136\,10^{-2}$	$1.0173\,10^{-2}$	$1.0306\,10^{-2}$	$1.0370\,10^{-2}$	$1.0417\,10^{-2}$
$x = 0.3$	$7.6494\,10^{-3}$	$7.6916\,10^{-3}$	$7.8468\,10^{-3}$	$7.9204\,10^{-3}$	$7.9755\,10^{-3}$
$x = 0.4$	$7.7562\,10^{-3}$	$7.8005\,10^{-3}$	$7.9672\,10^{-3}$	$8.0455\,10^{-3}$	$8.1046\,10^{-3}$
$x = 0.5$	$7.6186\,10^{-3}$	$7.6622\,10^{-3}$	$7.8326\,10^{-3}$	$7.9125\,10^{-3}$	$7.9728\,10^{-3}$
$\Delta x = 0.05$					
	$t = 6$	$t = 7$	$t = 8$	$t = 9$	$t = 10$
$x = 0.1$	$6.8993\,10^{-3}$	$6.9132\,10^{-3}$	$7.0141\,10^{-3}$	$7.0652\,10^{-3}$	$7.1014\,10^{-3}$
$x = 0.2$	$4.8407\,10^{-3}$	$4.8582\,10^{-3}$	$4.9962\,10^{-3}$	$5.0646\,10^{-3}$	$5.1135\,10^{-3}$
$x = 0.3$	$4.3007\,10^{-3}$	$4.3191\,10^{-3}$	$4.4793\,10^{-3}$	$4.5574\,10^{-3}$	$4.6136\,10^{-3}$
$x = 0.4$	$4.0345\,10^{-3}$	$4.0525\,10^{-3}$	$4.2250\,10^{-3}$	$4.3082\,10^{-3}$	$4.3684\,10^{-3}$
$x = 0.5$	$3.9534\,10^{-3}$	$3.9702\,10^{-3}$	$4.1465\,10^{-3}$	$4.2314\,10^{-3}$	$4.2928\,10^{-3}$
$\Delta x = 0.025$					
	$t = 6$	$t = 7$	$t = 8$	$t = 9$	$t = 10$
$x = 0.1$	$3.2177\,10^{-3}$	$3.2250\,10^{-3}$	$3.3278\,10^{-3}$	$3.3810\,10^{-3}$	$3.4179\,10^{-3}$
$x = 0.2$	$2.4010\,10^{-3}$	$2.4087\,10^{-3}$	$2.5487\,10^{-3}$	$2.6193\,10^{-3}$	$2.6688\,10^{-3}$
$x = 0.3$	$2.0193\,10^{-3}$	$2.0261\,10^{-3}$	$2.1885\,10^{-3}$	$2.2690\,10^{-3}$	$2.3258\,10^{-3}$
$x = 0.4$	$1.8360\,10^{-3}$	$1.8412\,10^{-3}$	$2.0161\,10^{-3}$	$2.1019\,10^{-3}$	$2.1627\,10^{-3}$
$x = 0.5$	$1.7815\,10^{-3}$	$1.7851\,10^{-3}$	$1.9641\,10^{-3}$	$2.0516\,10^{-3}$	$2.1137\,10^{-3}$

Table 1: Absolute errors $|\phi(x,t) - \phi_\theta^\infty(x)|$ evaluated for $\Delta t = 0.05$.

Remark 4. In Tab. 2, for different values of Δt, some computed values of $(\lambda_{\min}/\Delta t)\,T^2$, where $\lambda_{\min}$ is the minimum eigenvalue of $(A_{\mathscr{E}} + A_{\mathscr{E}}^\top)/2$ (i.e. the symmetric part of matrix $A_{\mathscr{E}}$) are reported. The problem taken into account is the Neumann wave propagation outside rectilinear obstacles of length $L = 0.2, L = 0.4$, respectively. We have fixed $\Delta x = 0.1$ for the spatial discretization and space-time piece-wise linear shape and test functions; the final observation times are $T = 10^{-3}$ and $T = 10^{-4}$. The obtained results are in agreement with what is stated in Remark 1 and Theorem 2.1. In fact, they represent the approximated coerciveness constant of the discretized energetic bilinear form for fixed Δx and vanishing Δt ($\lambda_{\min}$ must be divided by Δt in order to compare the discrete coerciveness constant with the theoretical one, with respect to the L^2 norm). This can be deduced also from the comparison between Tab. 2 and Tab. 3, where, for $L = 0.2, L = 0.4$ respectively, some computed values of the minimum eigenvalue of the symmetric part of the limit matrix (3.45), multiplied by $N_{\Delta t}^2 = (T/\Delta t)^2$, are reported.

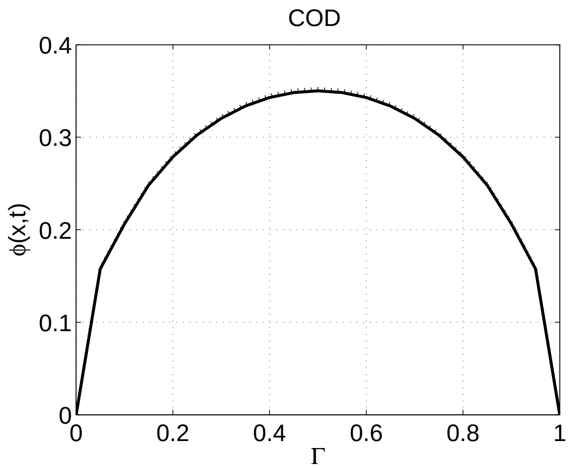

Figure 5: COD at $t = 4, 5, 10$ compared with static solution for $\theta = \pi/4$.

Due to all the above considerations, from a numerical point of view we can conjecture that also the coerciveness constant of the discretized energetic bilinear form behaves like $O(T^{-2})$, depending on the fixed crack length L.

Table 2: Behavior of $(\lambda_{\min}/\Delta t)\,T^2$, where $\lambda_{\min}$ is the minimum eigenvalue of $(A_{\mathscr{E}} + A_{\mathscr{E}}^{\top})/2$, for two different crack lengths

$T = 10^{-4}$			$T = 10^{-3}$		
Δt	$L = 0.2$	$L = 0.4$	Δt	$L = 0.2$	$L = 0.4$
10^{-5}	$1.3502\,10^{-1}$	$8.7286\,10^{-2}$	10^{-4}	$1.3504\,10^{-1}$	$8.7319\,10^{-2}$
10^{-6}	$1.6124\,10^{-1}$	$1.0424\,10^{-1}$	10^{-5}	$1.6144\,10^{-1}$	$1.0458\,10^{-1}$
10^{-7}	$1.6419\,10^{-1}$	$1.0616\,10^{-1}$	10^{-6}	$1.6619\,10^{-1}$	$1.0957\,10^{-1}$

Plane harmonic wave. As second example, we consider a wave which becomes harmonic after a fixed time (see [Becache (1993)]):

$$f(t) = \begin{cases} 0 & \text{if} \quad t < 0, \\ \dfrac{1}{2}(1 - \cos\omega t) & \text{if} \quad 0 \le t \le \dfrac{\pi}{\omega}, \\ \sin\left(\dfrac{\omega t}{2}\right) & \text{if} \quad t \ge \dfrac{\pi}{\omega}, \end{cases} \tag{4.51}$$

Table 3: Behavior of the minimum eigenvalue of the symmetric part of the limit matrix (3.45), multiplied by $N_{\Delta t}^2$, for two different crack lengths

$N_{\Delta t}$	$L = 0.2$	$L = 0.4$
10	$1.3502\,10^{-1}$	$8.7285\,10^{-2}$
100	$1.6124\,10^{-1}$	$1.0423\,10^{-1}$
1000	$1.6416\,10^{-1}$	$1.0612\,10^{-1}$

where ω represents the frequency. In this case the solution has to become harmonic too, with the same period as the incident wave, i.e. $P = 2\pi/\widetilde{\omega}$, where $\widetilde{\omega} = \omega/2$. The fixed circular frequency $\omega = 8\pi$ is such that the wave length $\lambda = 2\pi/\omega$ is equal to a quarter the crack length.
We choose a uniform decomposition of the crack Γ in 20 subintervals ($\Delta x = 0.05$) and we decompose the observation time interval $[0,10]$ in 400 equal parts ($\Delta t = 0.025$). For this numerical simulation we choose spatial linear shape and test functions.
In Fig. 6 we show the time harmonic behavior for $\theta = \frac{\pi}{2}$ of the crack opening displacement (COD) ϕ at $x = 0.4$, obtained starting from the energetic weak formulation. Note that the solution becomes immediately not trivial since the incident wave strikes the whole crack simultaneously. In Fig. 7 we present the approximated COD at instants $2,4,5,10$; the four curves overlap each other since the period is $P = 0.5$. In Fig. 8 we show the time harmonic behavior for $\theta = \frac{\pi}{3}$ of the crack opening displacement ϕ at $x = 0.4$. Note that the COD is zero till the time instant $t^* = cos(\theta)x = x/2$, since the incident wave, differently from the previous case, doesn't invest the whole crack simultaneously.

In order to verify that the period of ϕ coincides with the period of the incident wave, we show in Fig. 9 the approximate solution ϕ on Γ in time instants separated by multiples of the time period. Note that, after the first time instant taken under consideration, the three successive curves perfectly match each other.

Now, we present some results involving the total displacement field $u(\mathbf{x},t)$ obtained by the superposition of the incident wave $u^I(\mathbf{x},t)$ and the reflected and diffracted waves caused by the presence of a crack $\Gamma \subset \mathbb{R}^2$. The temporal profile of the incident wave, that strikes the crack and from which we have deduced the Neumann datum on Γ, is shown in Fig. 10 and it is similar to that one considered in [Iturraran-Viveros, Vai and Sanchez-Sesma (2005); Sanchez-Sesma and Iturraran-Viveros (2001)].

In the first simulation we deal with the crack $\Gamma = \{(x,0), x \in [-1,1]\}$ struck perpendicularly by the incident wave. The observation time interval is $[0,4]$. For the discretization, we fix a uniform subdivision of Γ in 40 elements ($\Delta x = 0.05$), the

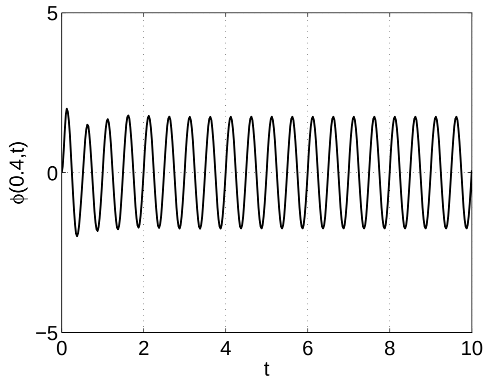

Figure 6: Density $\phi(0.4,t)$ for $\theta = \pi/2$.

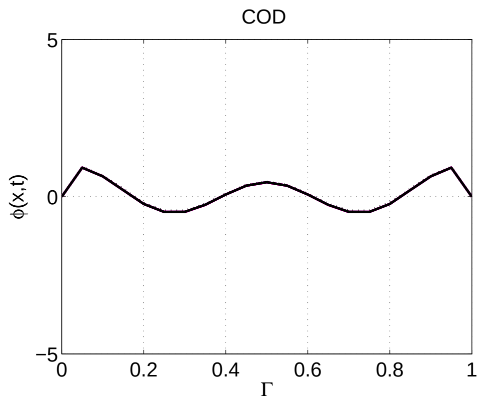

Figure 7: COD at $t = 2,4,5,10$ for $\theta = \pi/2$.

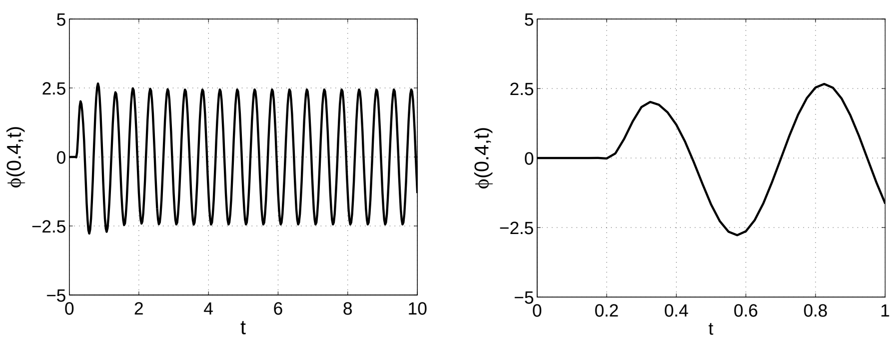

Figure 8: Density $\phi(x,t)$ calculated in $x = 0.4$ for $\theta = \pi/3$, with a zoom.

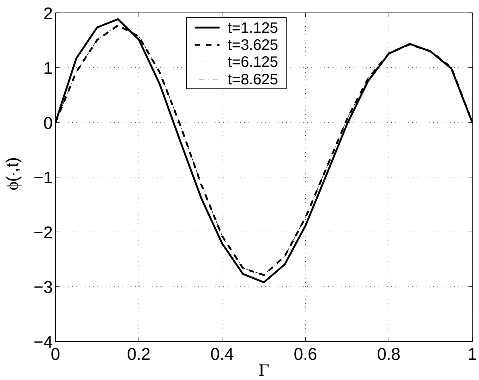

Figure 9: Solution $\phi(x,t)$ on Γ in different time instants separated by $5P$.

time step $\Delta t = 0.1$ and spatial linear shape and test functions.

In Fig. 11 we show the total recovered displacement in a square around the crack

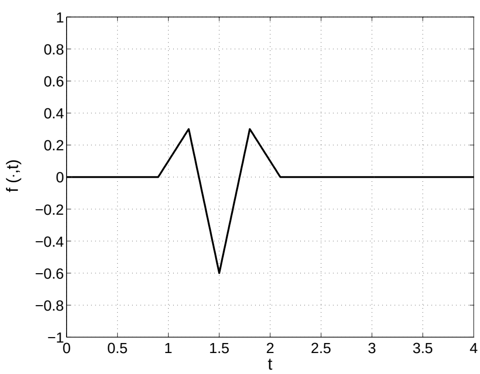

Figure 10: Temporal profile of the incident wave in the last five examples.

for different time instants. These results show how the plane wave reaches the crack and how the diffraction caused at the edges of the crack degenerates the wavefront. The effect of the diffraction on the upper half of the square creates a shadow. On the other hand, diffraction can be observed on the lower half of the square, too. Note that at the beginning of the simulation, the reflected wave on the upper half of the square cancel out with the incident wave. As time increases, the wavefront recovers and the scattering effect caused by the crack on the plane wave diminishes.

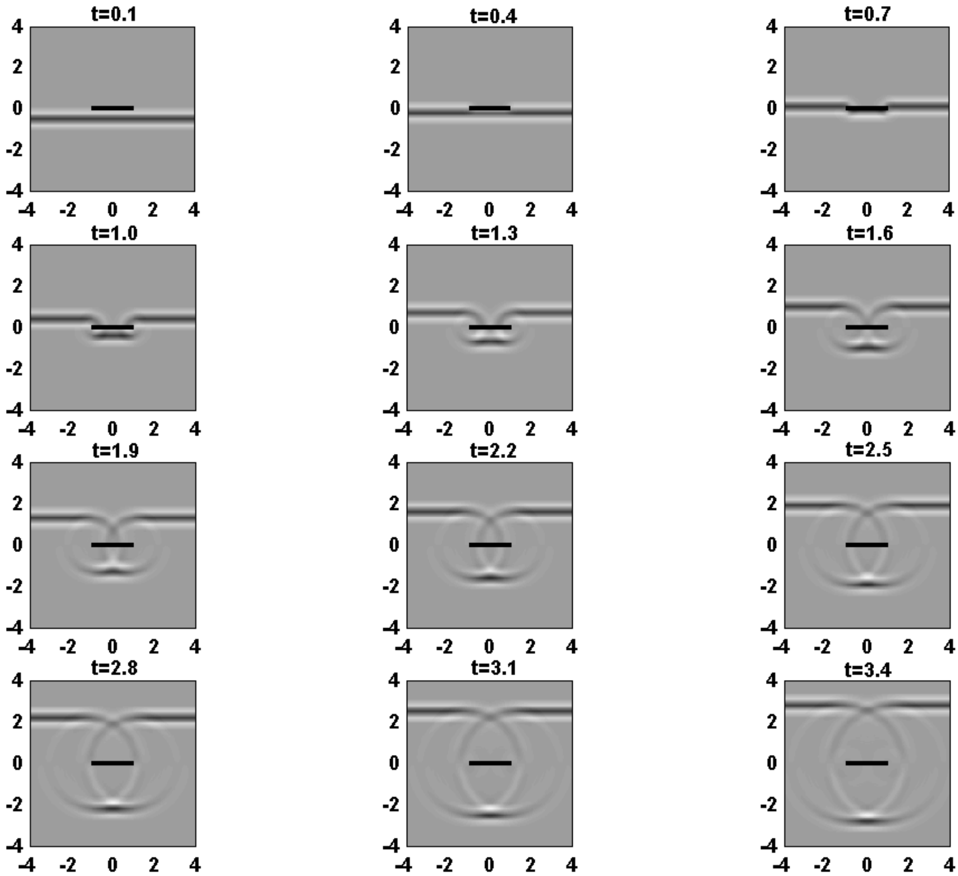

Figure 11: Total recovered displacement $u(\mathbf{x},t)$ around the straight crack.

In the second simulation we consider the semi-circular arc

$$\Gamma = \left\{ \mathbf{x} \in \mathbb{R}^2 : \mathbf{x} = (\cos\alpha, \sin\alpha), \alpha \in [0,\pi] \right\} ,$$

depending on the clockwise angle α, struck by the plane wave with an incident angle of amplitude $\frac{\pi}{3}$. The observation time interval is $[0,4]$. As uniform temporal discretization step we use $\Delta t = 0.1$ and Γ is uniformly approximated by 40 straight boundary elements where we adopt spatial linear shape and test functions. In Fig. 12 we show the total recovered displacement in a square around the crack for different time instants. We are able to identify at $t = 0.1$ the incident wave, at $t = 1.0$ the reflected wave, at $t = 1.6$ the first circular diffracted wave generated at the left edge of the crack, at $t = 2.5$ the first diffracted wave generated at the right edge of the crack.

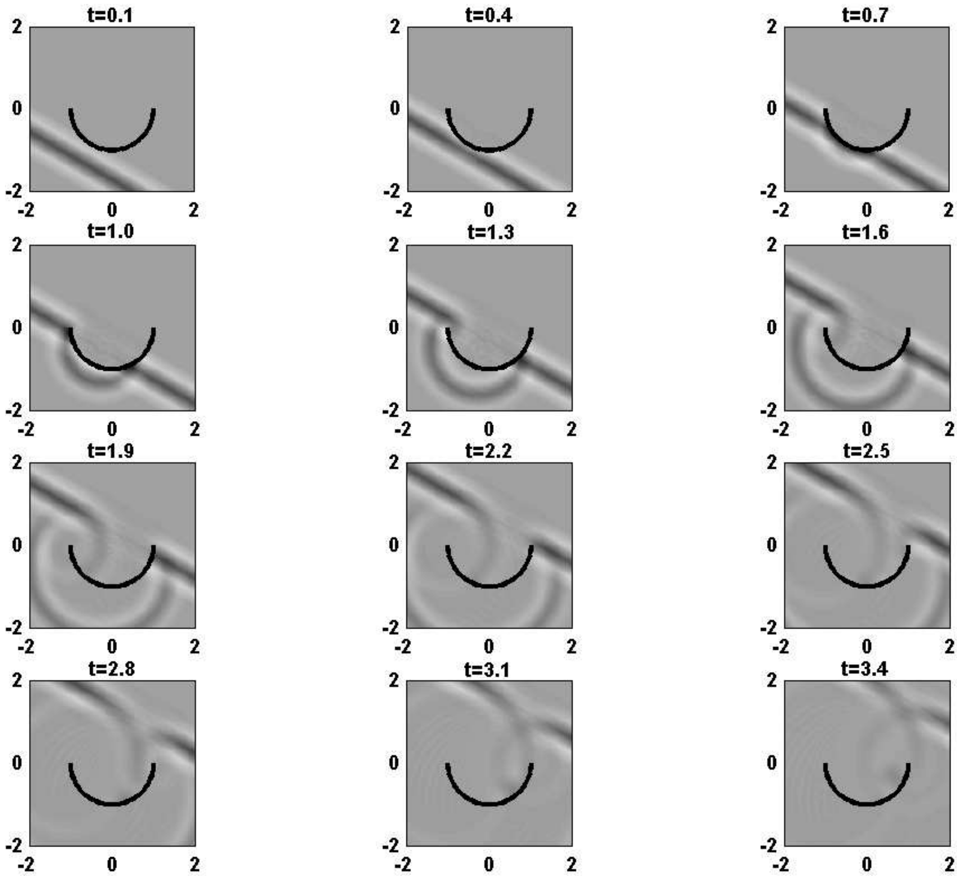

Figure 12: Total recovered displacement $u(\mathbf{x},t)$ around the semicircular crack.

In the third simulation we consider the curvilinear crack

$$\Gamma = \{\mathbf{x} \in \mathbb{R}^2 : \mathbf{x} = (0.5\,(\cos\alpha - 1), 0.5\,\sin\alpha) \vee (0.5\,(\cos(\alpha+\pi)+1), 0.5\,\sin(\alpha+\pi))\},$$

depending on the clockwise angle $\alpha \in [0,\pi]$, struck perpendicularly by the plane wave. The observation time interval is $[0,4]$. As uniform temporal discretization step we use $\Delta t = 0.1$ and Γ is uniformly approximated by 80 straight boundary elements where we adopt spatial linear shape and test functions. Several snapshots related to the total recovered displacement in a square around the crack for different time instants are shown in Fig. 13. The interesting part of the simulation is related to the incident wave "captured" by the right part of the crack and then reflected when the wavefront has already left the obstacle.

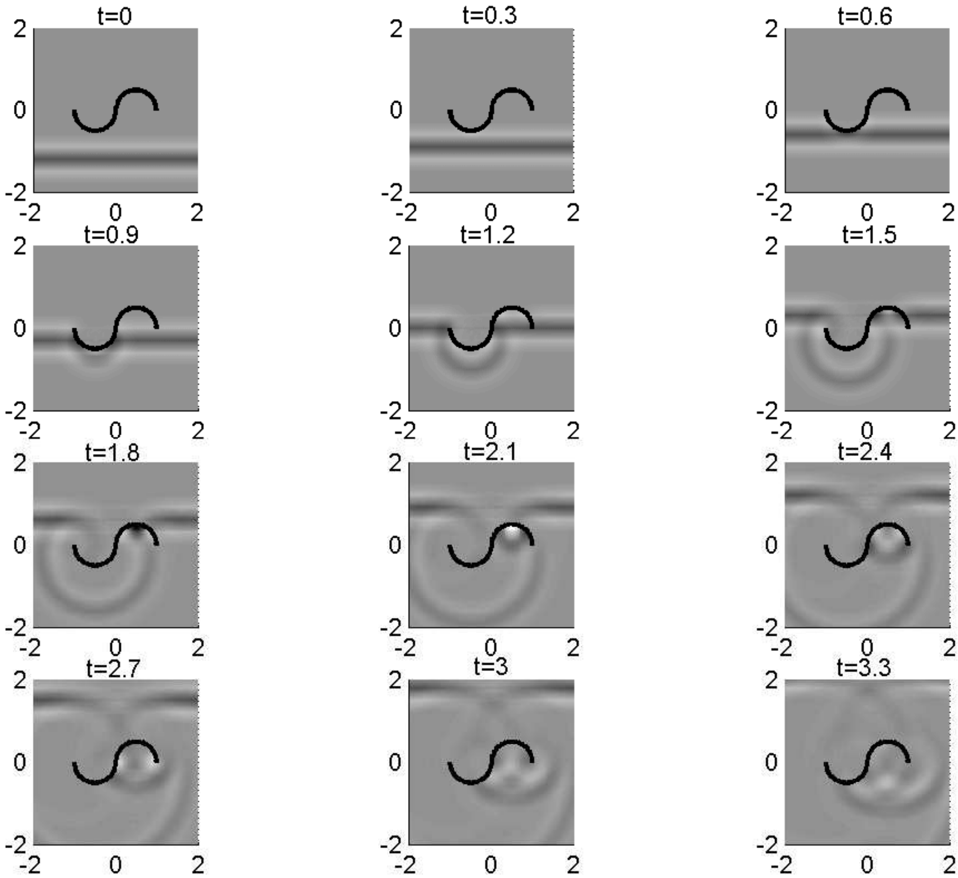

Figure 13: Total recovered displacement $u(\mathbf{x},t)$ around the curvilinear obstacle.

Energetic Galerkin BEM is now applied to two obstacles of different type with respect to the previous one. At first, the incident plane wave, shown in Fig. 10, strikes perpendicularly a breakwater obstacle, made by five disjoint aligned or parallel segments of length 0.5. The observation time interval is $[0,3]$. As uniform temporal discretization step we use $\Delta t = 0.1$ and every segment is uniformly approximated by 10 boundary elements ($\Delta x = 0.05$), where we adopt spatial linear shape and test functions. The total recovered displacement in a square around the obstacle for different time instants is shown in Fig. 14. As one can see, the adopted approximation technique furnishes satisfactory results also in the case of disconnected obstacles.

At last, the same incident plane wave strikes a unitary circle. The observation time interval is $[0,4]$. As uniform temporal discretization step we use $\Delta t = 0.1$ and the

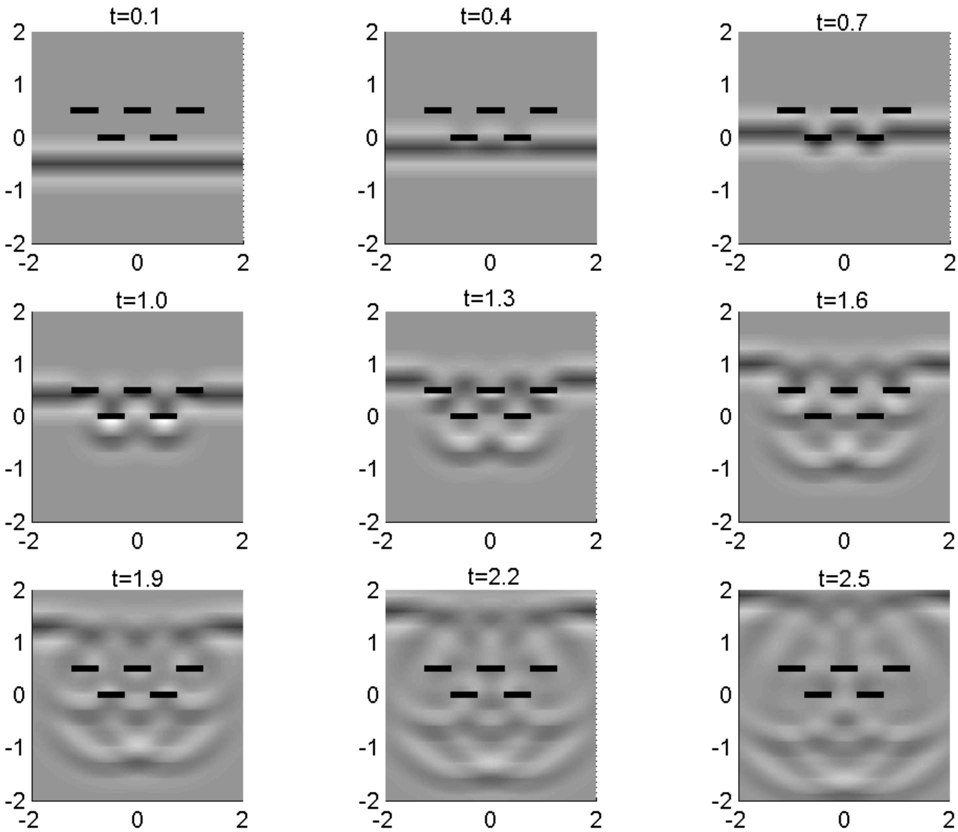

Figure 14: Total recovered displacement $u(\mathbf{x},t)$ around the brakewater obstacle.

boundary of the circle is uniformly approximated by 80 straight boundary elements where we adopt spatial linear shape and test functions. Several snapshots related to the total recovered displacement in a square around the plane convex domain for different time instants are shown in Fig. 15.

5 Conclusions

In this paper we have considered 2D wave propagation Neumann problems, exterior to different types of scatterers, reformulated in terms of a hypersingular BIE with retarded potential, which has been set in a suitable space-time energetic weak form. Galerkin BEM, applied to the energetic weak problem, has proved to be an efficient tool to obtained accurate approximate solutions. The analysis of the proposed technique has been conducted from both an analytical and a numerical point

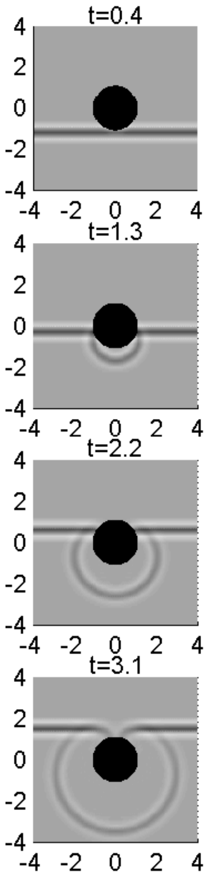

Figure 15: Total recovered displacement $u(\mathbf{x},t)$ around the circular obstacle.

of view, giving very satisfactory results.

Acknowledgement: This work has been partially supported by italian Ministero dell'Istruzione, dell'Unversità e della Ricerca (MIUR) under contract PRIN 2007JL35WY_002.

References

Aimi, A.; Diligenti, M.; Monegato, G. (1997): New Numerical Integration Schemes for Applications of Galerkin BEM to 2D Problems. *Int. J. Numer. Meth. Engng.*, vol. 40, pp. 1977–1999.

Aimi, A.; Diligenti, M.; Guardasoni, C.; Mazzieri, I.; Panizzi, S. (2009): An energy approach to space-time Galerkin BEM for wave propagation problems. *Int. J. Numer. Meth. Engng.*, vol. 80, pp. 1196–1240.

Aimi, A.; Diligenti, M.; Guardasoni, C. (2009): Numerical integration schemes for the discretization of BIEs related to wave propagation problems. In: J.Vigo-Aguiar (Ed.) *Proceedings of IX CMMSE Conference*, vol. I, pp. 45–56.

Aimi, A.; Diligenti, M.; Guardasoni, C. (2010): Numerical integration schemes for space-time hypersingular integrals in energetic Galerkin BEM. *Numerical Algorithms*, DOI: 10.1007/s11075-010-9371-3, in press.

Bamberger, A.; Ha Duong, T. (1986): Formulation variationnelle espace-temps pour le calcul par potentiel retardé de la diffraction d'une onde acoustique. I. *Math. Methods Appl. Sci.*, vol. 8, pp. 405–435.

Bamberger, A.; Ha Duong, T. (1986): Formulation variationnelle pour le calcul de la diffraction d'une onde acoustique par une surface rigide. *Math. Methods Appl. Sci.*, vol. 8, pp. 598–608.

Becache, E. (1993): A variational boundary integral equation method for an elastodynamic antiplane crack. *Int. J. Numer. Meth. Engng.*, vol. 36, pp. 969–984.

Becache, E.; Ha Duong, T. (1994): A space-time variational formulation for the boundary integral equation in a 2D elastic crack problem. *Math. Model. Numer. Anal.*, vol. 28, pp. 141–176.

Chandrasekhar, B.; Rao, S. M. (2005): Acoustic Scattering from Complex Shaped Three Dimensional Structures. *CMES: Computer Modeling in Engineering & Sciences*, vol. 8, pp. 105–117.

Chandrasekhar, B. (2005): Acoustic scattering from arbitrarily shaped three dimensional rigid bodies using method of moments solution with node based basis functions. *CMES: Computer Modeling in Engineering & Sciences*, vol. 9, pp. 243–253.

Costabel, M. (1994): Developments in boundary element methods for time-dependent problems. In: *Problems and methods in mathematical physics*. Teubner-Texte Math., vol. 134, pp. 17–32.

Costabel, M. (2004): Time-dependent problems with the boundary integral method. In Stein, E.; de Borst, R.; Huhes. T.J.R. (eds.): *Encyclopedia of Computational Mechanics*. Wiley, Chapter 25.

Frangi, A. (1999): Elastodynamics by BEM: a new direct formulation. *Int. J. Num. Meth. Engng.*, vol. 45, pp. 721–740.

Frangi, A. (2000): "Causal" shape functions in the time domain boundary element method. *Comput. Mech.*, vol. 25, pp. 533–541.

Fuchs, W. H. J. (1964): On the Eigenvalues of an Integral Equation Arising in the Theory of Band-Limited Signals. *J. Math. Analysis Appl.*, vol. 9, pp. 317–330.

Gallego, R.; Dominguez, J. (1996): Hypersingular BEM for transient elastodynamics. *Int. J. Numer. Meth. Engng.*, vol. 39, pp. 1681–1705.

Ha Duong, T. (1990): On the transient acoustic scattering by a flat object. *Japan J. Appl. Math.*, vol. 7, pp. 489–513.

Ha Duong, T. (2003): On retarded potential boundary integral equations and their discretization. In Davies, P.; Duncan, D.; Martin, P.; Rynne, B. (eds.): *Topics in computational wave propagation. Direct and inverse problems*. Springer-Verlag, pp. 301–336.

Ha Duong, T.; Ludwig, B.; Terrasse, I. (2003): A Galerkin BEM for transient acoustic scattering by an absorbing obstacle. *Int. J. Num. Meth. Engng.*, vol. 57, pp. 1845–1882.

Iturraran-Viveros, U.; Vai, R.; Sanchez-Sesma, F. J. (2005): Scattering of elastic waves by a 2-D crack using the Indirect Boundary Element Method (IBEM). *Geophys. J. Int.*, vol. 162, pp. 927–934.

Kielhorn, L.; Schanz, M. (2008): Convolution quadrature Method based symmetric Galerkin Boundary Element Method for 3-d elastodynamics. *Int. J. Numer. Meth. Engng.*, vol. 76, pp. 1724–1746.

Lebeau, G.; Schatzman, M. (1984): A wave problem in a half-space with a unilateral constraint at the boundary. *J. Differential Equations*, vol. 53, pp. 309–361.

Lubich, C. (1988): Convolution Quadrature and Discretized Operational Calculus. I. *Numer. Math.*, vol. 52, pp. 129–145.

Lubich, C. (1988): Convolution Quadrature and Discretized Operational Calculus. II. *Numer. Math.*, vol. 52, pp. 413–425.

Lubich, C. (1994): On the multistep time discretization of linear initial-boundary value problems and their boundary integral equations. *Numer. Math.*, vol. 67, pp. 365–389.

Miyatake, S. (1993): Neumann operator for wave equation in a half space and microlocal orders of singularities along the boundary. In: *Seminaire sur les Equations aux Derivees Partielles*, Exp. No. XVI, 8 pp., Ecole Polytech., Palaiseau, pp. 1992–1993.

Monegato, G.; Scuderi, L. (1999): Numerical integration of functions with boundary singularities. *J. Comput. Appl. Math.*, vol. 112, pp. 201–214.

Moser, W.; Antes, H.; Beer, G. (2005): Soil-structure interaction and wave propagation problems in 2D by a Duhamel integral based approach and the convolutive quadrature method. *Comput. Mech.*, vol. 36, pp. 431–443.

Patlashenko, I.; Givoli, D. (2000): Numerical Solution of Nonlinear Exterior Wave Problems Using Local Absorbing Boundary Conditions. *CMES: Computer Modeling in Engineering & Sciences*, vol. 1, pp. 61–70.

Premrov, M.; Spacapan, I. (2004): Solving exterior problems of wave propagation based on an iterative variation of local DtN operators. *Appl. Math. Model.*, vol. 28, pp. 291–304.

Sanchez-Sesma, F. J.; Iturraran-Viveros, U. (2001): Scattering and diffraction of SH waves by a finite crack: an analytical solution. *Geophys. J. Int.*, vol. 145, pp. 749–758.

Schanz, M; Antes, H.; Ruberg, T. (2005): Convolution quadrature boundary element method for quasi-static visco- and poroelastic continua. *Computers & Structures*, vol. 83, pp. 673–684.

Slepian, D. (1983): Some Comments on Fourier Analysis. *Uncertainty and Modelling*, SIAM Review, vol. 25(3), pp. 379–393.

Soares Jr., D.; Mansur, W. J. (2007): An efficient stabilized boundary element formulation for 2D time-domain acoustics and elastodynamics. *Comput. Mech.*, vol. 40, pp. 355–365.

Tadeu, A.; Godinho, L.; Antonio, J.; Amado Mendes, P. (2007): Wave propagation in the presence of empty cracks in elastic slabs - TDBEM and MFS Formulations. *ICCES*, vol. 3, pp. 163–168.

Zhang, Ch. (2002): A 2D hypersingular time-domain traction BEM for transient elastodynamic crack analysis. *Wave motion*, vol. 35, pp. 17–40.